Fibrinolytic Regulation of Pulmonary Epithelial Sodium Channels: a Critical Review

PhD candidate: Hong-Long (James) Ji

Mentors:

Dr. Tobias von der Haar

Professor Martin Michaelis

This work is submitted in partial fulfillment of the requirements of University of Kent for the degree of Doctor of Philosophy by Published Work

December 2015

Abstract

Luminal fluid homeostasis in the respiratory system is crucial to maintain the gas-blood exchange in normal lungs and mucociliary clearance in the airways. Epithelial sodium channels (ENaC) govern ~70% of alveolar fluid clearance. Four ENaC subunits have been cloned, namely, α, β, γ, and δ ENaC subunits in mammalian cells. This critical review focuses on the expression and function of ENaC in human and murine lungs, and the post-translational regulation by fibrinolysins. Nebulized urokinase was intratracheally delivered for clinical models of lung injury with unknown mechanisms. The central hypothesis is that proteolytically cleaved ENaC channels composed of four subunits are essential pathways to maintain fluid homeostasis in the airspaces, and that fibrinolysins are potential pharmaceutical ENaC activators to resolve edema fluid. This hypothesis is strongly supported by our following observations: 1) δ ENaC is expressed in the apical membrane of human lung epithelial cells; 2) δ ENaC physically interacts with the other three ENaC counterparts; 3) the features of αβγ ENaC channels are conferred by δ ENaC; 4) urokinase activates ENaC activity; 5) urokinase deficiency is associated with a markedly distressed pulmonary ENaC function *in vivo*; 6) γ ENaC is proteolytically cleaved by urokinase; 7) urokinase augments the density of opening channels at the cell surface; and 8) urokinase extends opening time of ENaC channels to the most extent. Our integrated publications laid the groundwork for an innovative concept of pulmonary transepithelial fluid clearance in both normal and diseased lungs.

Contents

Abstract 2

1. Introduction 6

The ENaC/DEG super gene family 7

Pulmonary fluid homeostasis 12

The urokinase system 15

2. Central Hypothesis 18

3. Significant Findings and Conclusions 19

3.1 Four epithelial sodium channels are expressed in human lung epithelium

3.1.1. Expression of δ ENaC protein in lung epithelial cells 19

3.1.2. Co-immunoprecipitation of α and γ ENaC with δ ENaC in H441 cells 20

3.1.3. Identification of a novel slicing variant for δ ENaC 20

3.2 δ ENaC confers the properties of αβγ ENaC channels

3.2.1. Cation permeability 21

3.2.2. Amiloride sensitivity 22

3.2.3. Unitary conductance 23

3.2.4. Gating kinetics 23

3.2.5. Proton activation 24

3.2.6. Self-inhibition 24

3.2.7. Dependence of P_{Na}/P_{Li} ratio and unitary Na^+ conductance on injected cRNA concentrations 25

3.3 Urokinase contributes to fluid homeostasis in pulmonary system

3.3.1. Characterization of ENaC activity in *uPA* knockout cells 26

3.3.2. Reduction of ENaC activity in *uPA*-deficient MTE cells 27

3.3.3. *uPA* deficiency down-regulates ENaC activity in permeabilized cells 28

3.3.4. Phosphorylation of ERK1/2 and Akt by uPA 28

3.3.5. Apoptosis is not involved in the reduction of ENaC activity 29

3.3.6. Proteolysis of ENaC by uPA 30

3.3.7. Contribution of uPA to airway luminal fluid homeostasis 31

3.4 Urokinase plasminogen activator proteolytically cleaves γ ENaC subunits

3.4.1. γ ENaC is cleaved by uPA 32

3.4.2. Identification of cleavage regions in ENaC 32
3.4.3. An uPA substrate in γ ENaC 34
3.5 Localization of “cutting edge” of urokinase to catalyze ENaC
3.5.1. uPA but not tPA activates ENaC 35
3.5.2. Catalytic triad of uPA to cleave ENaC 37
3.5.3. Structural interactions between catalytic sites of uPA and cleavage sites of γ ENaC 38
3.6 Urokinase augments opening channel density and opening time of channels
3.6.1. uPA strengthens the open conformation of ENaC 40
3.6.2. uPA activates “silent” channels 41
3.6.3. uPA optimally increases opening time 41
3.7 Proteolysis is the mechanism to elevate ENaC activity to the utmost level vs self-inhibition releasing agents
3.7.1. cpt-cAMP cannot activate cleaved ENaC by fibrinolysin 43
3.7.2. Cleavage abolishes cpt-cAMP-mediated ENaC activation in human lung epithelial cells 44
3.7.3. CPT-cGMP ligand docking to different ENaC domains 44
3.7.4. CPT-cGMP and self-inhibition 45
3.7.5. Specific self-inhibition domains differ from uPA cleavage sites 46
3.7.6. Self-Inhibition as an alternative approach to fibrinolysins 47
4. Theoretical Framework
4.1. How and in what respect the work has made a significant and coherent contribution to knowledge 48
4.2. Impact 49
4.3. Methodologies 50
5. Summary/Conclusions 51
6. Contributions made by the candidate 53
7. Bibliography 59

Figure 1 6
Figure 2 8
Figure 3 10
Figure 4 11
Figure 5 14
Figure 6 29

Figure 7 39
Figure 8 51

1. Introduction

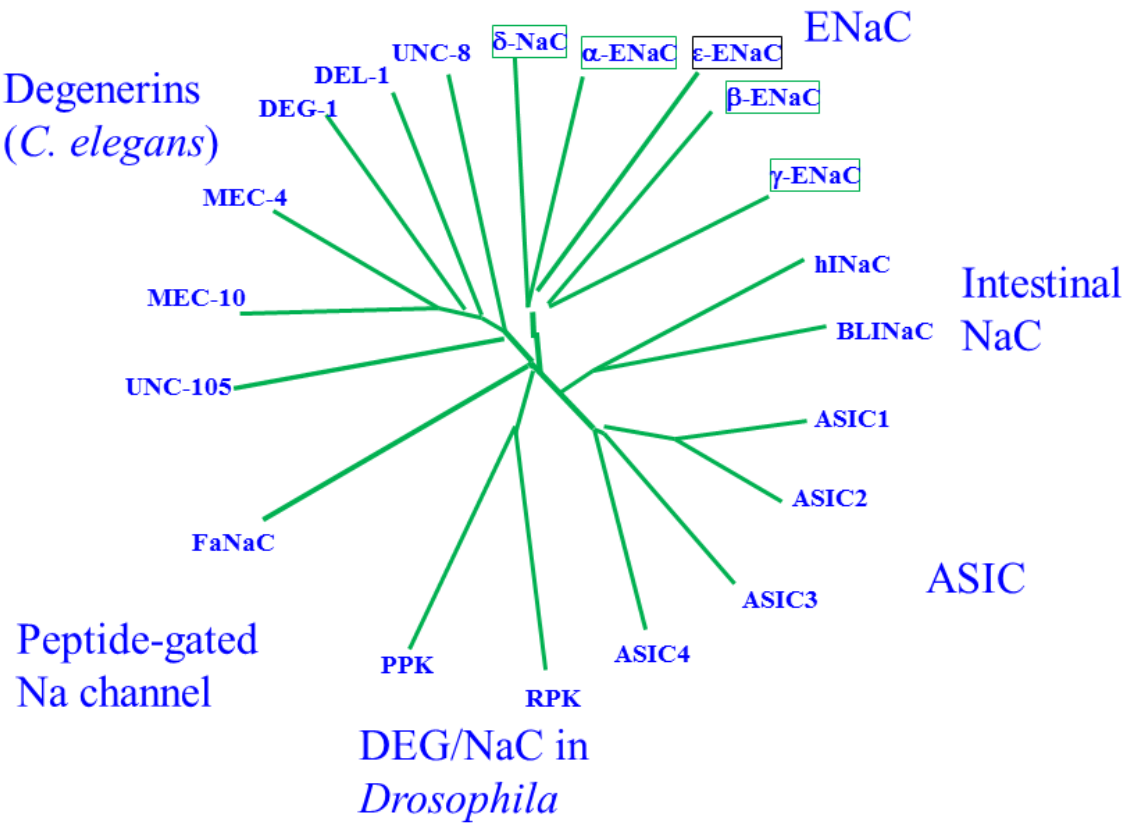

Figure 1. Polygenetic tree of the ENaC/DEG superfamily. ENaC, epithelial sodium channels; ASIC, acid sensing ion channels; NaC, sodium channels; DEG, degenerins.

This review explores a central thread in the ideas and publications generated in the last two decade by myself and by prolific collaborations with my colleagues. I initiated my studies in amiloride-sensitive epithelial sodium transport in 1995 while I was trained as a postdoctoral fellow in the University of Georgia at Athens. I extended my research to understand the structure-function relationship of α, β, and γ ENaC combining mutagenesis and heterologous expression in a well-established 3-D cell model, *Xenopus* oocytes. Subsequently, I cloned three DNA constructs encoding δ

ENaC subunits in human lungs (Ji *et al.*, 2006; Zhao *et al.*, 2012), and characterized their biophysical and pharmacological features and expression profiles in human lungs (Ji *et al.*, 2006; Zhao *et al.*, 2012). I recently found that fibrinolysins in bronchioalveolar lavage are critical regulators of ENaC function. I, for the first time, identified both the cleavage sites in human ENaC proteins and the catalytic triad of urokinase (Ji *et al.*, 2015). This review will summarize the critical findings of these publications.

The ENaC/DEG super gene family. Human ENaC subunits (α, β, δ, and γ) are encoded, respectively, by four genes, namely, *scnn1a* (sodium channels nonvoltage-dependent), *scnn1b*, *scnn1d*, and *scnn1d*. These genes are comprised of a branch of the super ENaC/DEG gene family with more than a hundred members (Figure 1). The name degenerin (DEG) comes from the cellular phenotype induced by mutations of *deg*-1 and other related genes that result in selective degeneration of sensory neurons involved in touch sensitivity of *C. elegans* (Kellenberger & Schild, 2002). ENaC and degenerins have substantial sequence homology. The *scnn1* genes encoding ENaC proteins were first cloned from mouse colon in 1993 (Canessa *et al.*, 1993). Before that, there are several names for this type of channels, *e.g.*, amiloride-sensitive sodium channels, voltage-independent sodium channels, non-voltage-gated sodium channels, amiloride-inhibitable sodium channels, apical sodium channels, etc. to form leaking sodium permeation pathway across the apical membrane of polarized epithelium in the kidney, the lung, the airways, the colon, the sweat gland, and other tissues. The essential function of ENaC is to serve as cation channels with a permeability order: $Li^+ > Na^+ > K^+ > Cs^+$. Beside, ENaC as well as other members of the ENaC/DEG family are also expressed in non-epithelial cells, including neurons, smooth muscle cells,

leukocytes, endothelial cells, cardiovascular myocytes, mesothelial cells, and skin

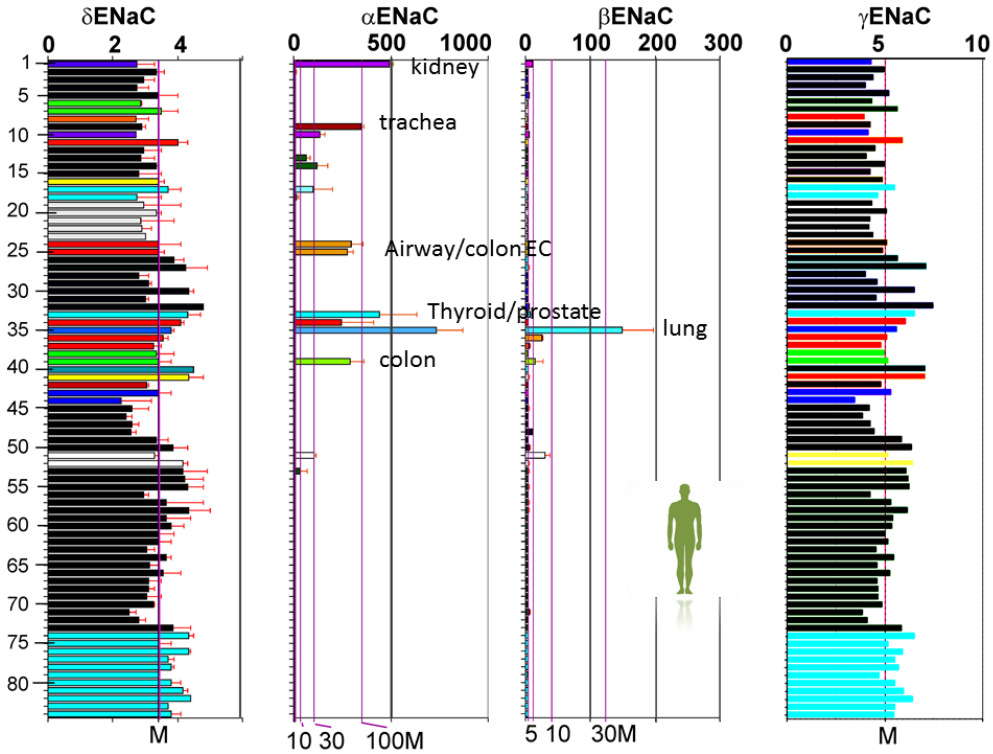

Figure 2. Gene expression profile of *scnn1a*, *scnn1b*, *scnn1g*, and *scnn1d*. Expression levels are computed from the "GeneAtlas U133A, gcmas" dataset, an atlas of tissue expression (GeneAtlas) on an Affymetrix U133A array, using the gcrma algorithm to process the data. The *y*-axes on these graphs represent normalized, background-subtracted, and summarized (probes to probeset) intensity of each probe set: 1 kidney, 2 tonsil, 3 lymph node, 4 thymus, 5 bone marrow, 6 adrenal gland, 7 adrenal cortex, 8 olfactory bulb, 9 trachea, 10 salivary gland, 11 pituitary, 12 fetal liver, 13 fetal lung, 14 fetal thyroid, 15 uterus, 16 adipocyte, 17 pancreatic islet, 18 pancreas, 19 testis seminiferous tubule, 20 testis Leydig cell, 21 testis interstitial, 22 testis germ cell, 23 testis, 24 colorectal adenocarcinoma, 25 bronchial epithelial cells, 26 smooth muscle, 27 cardiac myocytes, 28 leukemia lymphoblastic (MOLT-4), 29 leukemia chronic myelogenous K-562, 30 lymphoma Burkitts (Daudi), 31 leukemia promyelocytic HL-60, 32 leukemia Burkitts (Raji), 33 thyroid, 34 prostate, 35 lung, 36 placenta, 37 CD71+ early erythroid, 38 small intestine, 39 colon, 40 liver, 41 heart, 42 uterus corpus, 43 appendix, 44 ovary, 45 dorsal root ganglion, 46 ciliary ganglion, 47 atrioventricular node, 48 skin, 49 trigeminal ganglion, 50 superior cervical ganglion, 51 tongue, 52 skeletal muscle, 53 retina, 54 pineal night, 55 pineal day, 56 whole brain, 57 amygdala, 58 prefrontal cortex, 59 spinal cord, 60 hypothalamus, 61 fetal brain, 62 thalamus, 63 caudate nucleus, 64 parietal lobe, 65 medulla oblongata, 66 cingulate cortex, 67 occipital lobe, 68 temporal lobe, 69 subthalamic nucleus, 70 pons, 71 globus pallidus, 72 cerebellum, 73 cerebellum peduncles, 74 CD34+, 75 CD105+ endothelial, 76 721 B lymphoblasts, 77 CD19+ B cells (neg._sel.), 78 BDCA4+ dendritic cells, 79 CD8+ T cells, 80 CD4+ T cells, 81 CD56+ NK cells, 82 CD33+ myeloid, 83 CD14+ monocytes, 84 whole blood. The bottom *x*-axes show the median (M) and the fold median level, as indicated by purple lines, and the top *x*-axes show the relative expression level with light gray lines; 176 samples for 84 types of tissues were statistically analyzed. These results represent relative expression levels and distribution of four *scnn1* genes in human tissues. *Scnn1a* and *scnn1b* are predominately expressed in the lungs, while the other genes are distributed in 84 examined tissues/cells without marked difference. Data are adapted from BioGPS with permission (www.BioGPS.org). Adapted from Ji, et al 2012.

(Figure 2). Their function in non-epithelial tissues is proposed to be involved in acid sensing, transduction of mechanical stimuli, and nociceptive pain (Ji *et al.*, 2012).

ENaC is a multimeric protein with a proposed heterotrimeric structure (Figure 3) (Jasti *et al.*, 2007). However, our understanding of the architecture of the native ENaC proteins is incomplete. Based on heterologous expression studies, α and δ ENaC subunits are capable of forming electrically detectable channels, which will be amplified up to 2 order in the amplitude of current levels by co-expressing with β and γ counterparts. In contrast, in the absence of α or δ ENaC subunit, β and γ ENaC cannot form functional channels and are considered as regulatory subunits. So far, *scnn1* genes have been cloned from various species, such as rat, human, cow, mouse, and *Xenopus laevis.* For experimental clarity, murine and human ENaC channels are well investigated and widely used as research models. The homology between human and rat orthologs of ENaC subunit is about 85% to nearly 100%. The exon–intron architecture of the four genes encoding the four subunits of ENaC has remained highly conserved despite the divergence of their sequences (Kellenberger & Schild, 2002). The proteins that belong to the ENaC/DEG family consist of about 510 to 920 amino acid residues (Kellenberger & Schild, 2002; Ji *et al.*, 2012). They are made of an intracellular N-terminus region followed by a transmembrane domain, a large extracellular loop contributing to approximate 60% of protein mass, a second transmembrane segment and a cytosolic C-terminal tail (Figure 3) (Ji *et al.*, 2012). Few sequences are completely conserved among the ENaC/DEG family. They include a His-

Glycine motif located in amino-terminal cytoplasmic domain and the extracellular loop contains cysteine rich domains II and III (Kellenberger & Schild, 2002).

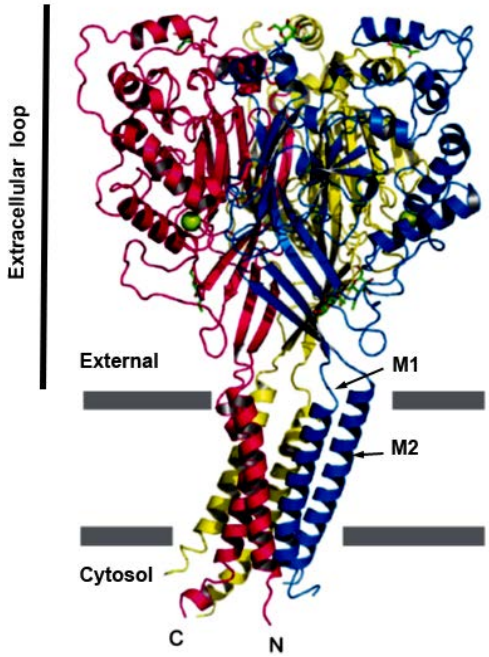

Figure 3. Heterotrimeric structure of ENaC proteins. α, β, and γ ENaC subunits are in red, yellow, and blue color, respectively. The lipid bilayer of the plasma membrane are shown as dark lines in parallel. There are two transmembrane domains (M1 and M2), two intracellular terminal tails (N- and C-), and a huge extracellular loop. Adapted from Ji et al 2016.

ENaC channels are located in the apical membrane of polarized epithelial cells particularly in the kidney, the lungs, and the colon where they mediate Na^+ transport across tight epithelium. ENaC pathway plays a major role in Na^+ and K^+ ion homeostasis of blood, epithelia and luminal fluids by re-absorption of Na^+ ions (Stockand *et al.*, 2008). The basic functions of ENaC in polarized epithelial cell are to allow vectorial transcellular transport of Na^+ ions (Figure 4) (Rossier & Stutts, 2009). This transepithelial Na^+ ion transport through a cell basically involves two steps: first, the large electrochemical gradient for Na^+ ions across the apical membrane provides the driving force for the entry of Na^+ into the cell and second, active Na^+ transport

across the basolateral membrane is accomplished by the energy-consuming Na^+/K^+-

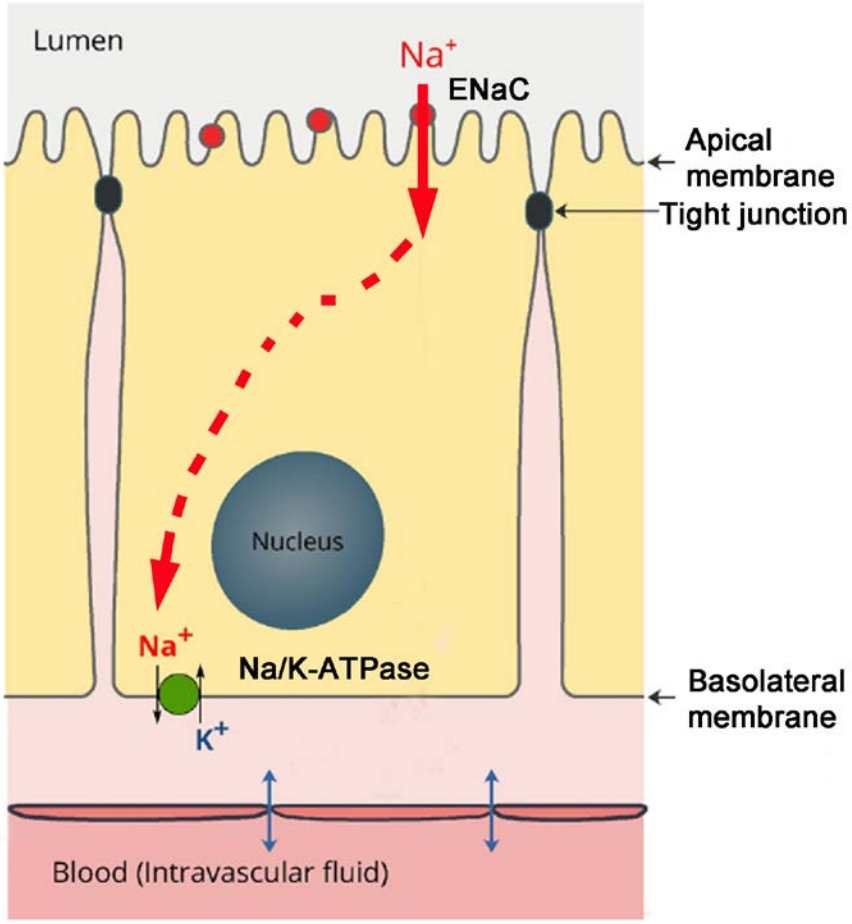

Figure 4. Transepithelial Na^+ transport vectorially across apically located ENaC and Na^+/K^+-ATPase at the basolateral membrane. Adapted from Hanukoglu 2016 (Hanukoglu & Hanukoglu, 2016).

ATPase (Rossier & Stutts, 2009). The apical entry of Na^+ is blocked by submicromolar concentration of amiloride and analogs, which are used as potassium-sparing diuretics clinically. Amiloride directly "plugs in" the pore of ENaC channels to eliminate inward sodium flow (Kleyman & Cragoe, 1988; Kleyman *et al.*, 1999). Inhibition of renal ENaC activity leads to a loss of sodium retention and subsequently dehydration of the body, and even causes hypotension. Amiloride is a competitive antagonist that competes with aldosterone for intracellular cytoplasmic receptor sites, or by directly blocking ENaC channels. This active transepithelial transport of Na^+ ions is important for maintaining

the composition and the volume of the fluid on either side of the epithelium. In the kidney and the colon, which are the target tissues for aldosterone action, the transepithelial sodium transport is crucial for the maintenance of blood Na^+ and K^+ levels and their homeostasis. In the airways and the lungs, active transepithelial transport of Na^+ ions is a major mechanism to keep the mucociliary beating of the ciliated epithelial cells and to prevent flooding of the air spaces.

Pulmonary fluid homeostasis. The airway epithelia absorb Na^+ via an amiloride-sensitive electrogenic transport. This active Na^+ absorption is important for the maintenance of the composition of the airway surface liquid (Figure 4). The expression of the ENaC subunits along the respiratory epithelium is complex and varies between species. In adult rats and humans, the α, β, and γ ENaC subunits are highly expressed in small and medium-sized airways. The α and γ subunits but not the β subunits are expressed more distally in the lung, which may well correspond to localization in the type II alveolar cells. This heterogeneity of the expression of ENaC subunits along the airways suggests differential regulation of liquid absorption by channels of various subunit compositions (Matalon & O'Brodovich, 1999).

At birth, amiloride-sensitive, electrogenic Na^+ transport is important to clear the liquid that fills the alveoli and the airways of the fetal mouse lung. mRNAs for α, β, and γ ENaC were detected in the fetal lung around days 15–17 of gestation. Expression of ENaC subunits, mainly α and γ ENaC subunits, sharply increased in the late fetal and early postnatal life when the lung turned from a secretory to an absorptive organ (Thome *et al.*, 2003). The physiological role of ENaC in lung liquid balance was clearly

demonstrated in mice in which the α ENaC gene was inactivated by homologous recombination. These α ENaC knockout mice died 48 hours after birth from respiratory failure due to a severe defect in the clearance of the fetal liquid filling the lungs. These studies suggest that at birth α ENaC in the mouse fetal lung is essential for Na^+ absorption (Hummler *et al.*, 1996). The disruption of the β and γ ENaC gene loci resulted in a slower clearance of the fetal lung liquid at birth but did not severely affect the blood gas parameters. The β or γ ENaC knockout mice died slightly later than the α knockout from severe electrolyte imbalance, namely, hyperkalemia due to deficient renal K^+ secretion. In humans, the contribution of α ENaC to the clearance of fetal lung liquid at birth is still unclear. Very premature infants with respiratory distress syndrome had reduced sodium absorption across the respiratory epithelia, as demonstrated by a reduced nasal transepithelial potential difference, likely contributing to the pathogenesis of this syndrome. However, pseudohypoaldosteronism type I (PHA-I) patients with severe disruption of the α ENaC gene leading to near-complete loss of channel function had no report of respiratory distress syndrome at birth but showed a more than twofold higher liquid volume in airway epithelia than normal individuals. Thus, ENaC function in humans does not seem to be limiting at birth for the liquid clearance in the mature fetal lung. Differences between species in maturation of the lung, in mucociliary clearance, or in ENaC subunit expression in the respiratory epithelium may account for the phenotypic differences between humans and mice.

Of note, mice do not express δ ENaC because the *scnn1d* is a pseudogene in murine. In sharp contrast to the early death of newborn litters of *scnn1a* knockout mice,

infants carrying a loss-of-function mutant of human α ENaC did not display a deadly distress syndrome caused by lung oedema (Trautmann & Pfeiffer, 1994; Bonny *et al.*, 1999), indicating that δ ENaC subunit may be a backup of α ENaC counterpart (Ji *et al.*, 2012). However, surviving children with the genetic deletion of *scnn1d*, encoding δ ENaC proteins, were predisposed to respiratory oedematous disorders and infection (Unique, 2008). In addition, numerous pathogens and pollutants decreased ENaC expression and function *in vitro* and *in vivo* (Ji *et al.*, 2012). On the other hand, cystic fibrosis is a phenotype with hyperactive ENaC activity in the airways and the lungs. Genetically engineered mice over-expressing either α, β, γ, or all of three (α+β+γ) ENaC

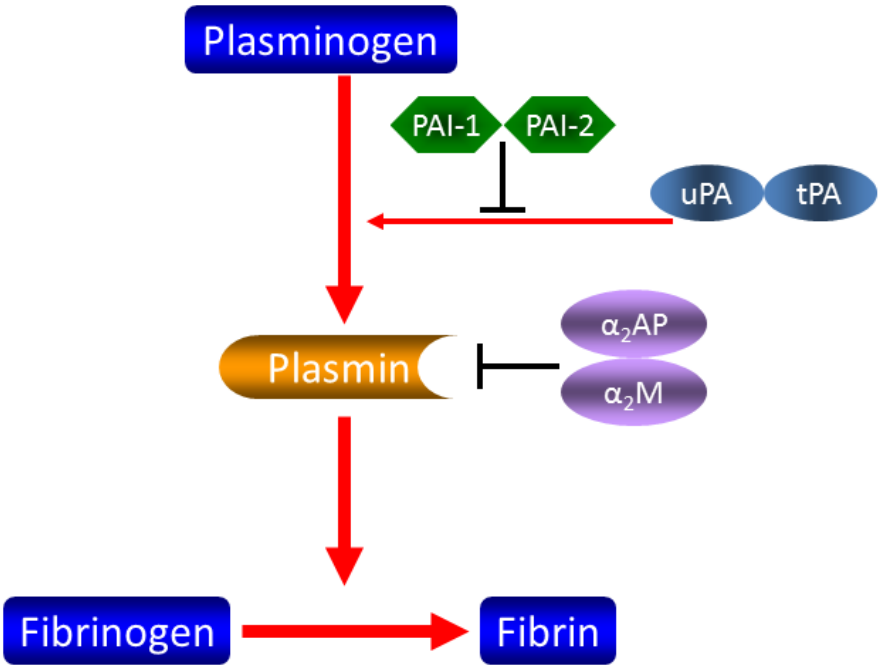

Figure 5. The uPA system. uPA, urokinase; tPA, tissue-type plasminogen activator; α2-AP, α2-antiplasmin; α2-M, α2-macroglobulin; PAI, plasminogen activator inhibitor.

subunits had a COPD as well as cystic fibrosis phenotypes (Mall *et al.*, 2004; Zhou *et al.*, 2007; Mall *et al.*, 2008; Zhou *et al.*, 2011).

The urokinase system. Urokinase-type plasminogen activator (uPA) initiates fibrinolysis by converting plasminogen to plasmin (Figure 5). In the respiratory system, uPA is expressed in the airway epithelium, alveolar epithelial cells, macrophages, and pulmonary capillary endothelial layer (Gross *et al.*, 1990; Marshall *et al.*, 1990; Takahashi *et al.*, 1992; Nishiuma *et al.*, 2004; Sisson & Simon, 2007; Shetty *et al.*, 2008). uPA released from these cells is a single-chain molecule (scuPA), which can be further proteolytically cleaved to form active two-chain enzyme (tcuPA). uPA is readily detectable in bronchioalveolar lavage and pleural fluid in mammals, and is a primary contributor of fibrinolytic activity in lungs (Chapman *et al.*, 1986; Kotani *et al.*, 1995; Nishiuma *et al.*, 2004). Tissue-type plasminogen activator (tPA), however, is not expressed in lung epithelial tissues and cannot be detected in luminal fluid lining the airways and air sacs. Both uPA and tPA are endogenous plasminogen activators. To maintain fibrinolytic homeostasis, inhibitors of plasminogen activators 1 and 2 (PAI-1 and PAI-2) and plasmin (α2-antiplasmin and α2-macroglobulin) coordinately fine tune the plasminogen activation system.

The balance between plasminogen activators and their corresponding inhibitors is disrupted in oedematous lungs and pleural injuries, including ALI, ARDS, high altitude pulmonary oedema, and pleural effusions (Idell, 2008; Shetty *et al.*, 2008; Glas *et al.*, 2013). Accumulating evidence from clinical studies of premature infants with ARDS and animal models of pleural effusions and ALI confirmed a depression in plasminogen activation in bronchioalveolar lavage or pleural fluid (Idell *et al.*, 1992a; Idell *et al.*,

1992b; Viscardi *et al.*, 1992). This is primarily attributable to a tremendous elevation in PAI-1 level (a prognostic biomarker) and a significant reduction in uPA and plasmin (Bertozzi *et al.*, 1990; Idell *et al.*, 1991; Sisson *et al.*, 2002; Prabhakaran *et al.*, 2003; Sapru *et al.*, 2010). Concurrently, the balance between fluid turnover and resolution in the airways, alveolar spaces, and pleural cavity is lost. Accumulation of oedematous fluid mainly results from fluid re-absorption that cannot be compensated by fluid leakage (Matthay *et al.*, 2002; Davis & Matalon, 2007; Eaton *et al.*, 2009). This pathogenic scenario can be illustrated with alveolar fluid clearance. Alveolar fluid removal is driven by the osmotic sodium gradient as well as electrical potential difference across the alveolar epithelium. Vectorial transalveolar salt transport generates both chemical and electrical differences between luminal and interstitial compartments. Epithelial sodium channels (ENaC) at the apical membrane and ATP-consuming Na^+/K^+-ATPase at the basolateral membrane coordinately control sodium inward movement and depolarize the epithelial layer (Fuller *et al.*, 1996; Ji *et al.*, 2012).

Reduced ENaC expression and activity were described in both oedematous pulmonary diseases and animal models (Matthay *et al.*, 2002; Matthay, 2014). Defective lung fluid clearance has been confirmed in mice with deficient *scnn1* genes (Hummler & Planes, 2010). uPA and tPA decreased the severity of lung injury and pleural effusions (Strange *et al.*, 1995; Stringer *et al.*, 1998; Munster *et al.*, 2000; Stringer *et al.*, 2004; Renckens *et al.*, 2008; Huang *et al.*, 2012; Komissarov *et al.*, 2013). Whether delivered plasminogen activators evoke ENaC-mediated oedema resolution, however, is unknown to date.

The concurrent oedema formation and suppressed fibrinolysis in injured lungs

and pleural cavity, suggest a potential contribution of fibrinolysis to ENaC function. Indeed, ENaC activation by plasmin has been recently demonstrated (Passero *et al.*, 2008; Haerteis *et al.*, 2012). Intratracheal and intrapleural delivery of uPA (abbokinase) and tPA (alteplase) is extensively used for fibrinolytic therapy for embolisms (Wang *et al.*, 2010; Marhuenda *et al.*, 2014; Meyer *et al.*, 2014; Piazza *et al.*, 2015), pleural effusions, and empyemas (Diacon *et al.*, 2004; Cases Viedma *et al.*, 2006; Thommi *et al.*, 2007; Froudarakis *et al.*, 2008; Zuckerman *et al.*, 2009; Rahman *et al.*, 2011; Thommi *et al.*, 2012; Aleman *et al.*, 2015; Cao *et al.*, 2015; Saydam *et al.*, 2015). However, to the best of our knowledge, the effects and underlying mechanisms of tPA and uPA on ENaC function remain obscure. Our studies therefore aim to understand the molecular and pharmacological mechanisms by which these serine proteases resolve oedema fluid.

2. Central Hypothesis that links published works

The central hypothesis that links my previous publications is that δ subunit-containing channels are essential to maintain pulmonary fluid homeostasis and fibrinolysins post-translationally cleave ENaC to regulate transepithelial salt re-absorption. Our published data strongly support this hypothesis as described in Section 3. These studies were performed *in vitro*, *in vivo* and *ex vivo* with multiple cutting-edge techniques. The main goal of our projects is to characterize the major pathway of fluid clearance *via* ENaC and the regulation by fibrinolysis. We thus aim to confirm that 1) a novel δ ENaC contributes to pulmonary epithelial sodium transport; 2) fibrinolysis regulates ENaC-mediated fluid homeostasis under physiological conditions; 3) the uPA pathway regulates normal ENaC function; and 4) molecular mechanisms for fibrinolysins to activate ENaC. Our published works strongly support this central hypothesis. Our data provide paradigm-shifting information to develop innovative therapeutic strategies for combating both “wet” and “dry” lungs.

3. Significant Findings and Conclusions

3.1 Four epithelial sodium channels are expressed in human lung epithelium

Three ENaC subunits were first identified in mice in 1994 (Canessa *et al.*, 1994). Thereafter, it has long been accepted that the native ENaC channels are composed of α, β, and γ subunits. The expression and function of δ ENaC subunits in the respiratory system has not yet been paid enough attention given the fact that α ENaC deficiency resulted in death of newborn mice. On the other hand, mice do not express δ ENaC (Ji *et al.*, 2012). Furthermore, over expression of β ENaC caused a postnatal death due to developmental deficiency of the respiratory system (Mall *et al.*, 2004). We thus hypothesize that δ ENaC may be a critical components of human pulmonary ENaC channels.

3.1.1. Expression of δ ENaC protein in lung epithelial cells. H441 is an airway epithelial cell line derived originally from human stem cells, Club or Clara epithelial cells. It has been used to functionally study amiloride-sensitive sodium channels associated with ENaC in several groups, including us (Tucker *et al.*, 1998; Kulaksiz *et al.*, 2002; Lazrak & Matalon, 2003; Ji *et al.*, 2006; Nie *et al.*, 2009a; Han *et al.*, 2010; Han *et al.*, 2011). To detect δ ENaC expression at the protein level, H441 monolayers grown on filters were immunostained with a specific anti- δ ENaC antibody, followed by a FITC conjugated secondary antibody. We found the expression of δ ENaC in H441 cultures (Ji *et al.*, 2006). α, β, and γ ENaC proteins were also detected in H441 monolayers, in agreement with other studies (Wodopia *et al.*, 2000; Itani *et al.*, 2002).

Cells incubated with non-immune IgG and the secondary antibody did not exhibit immunofluorescence. Similar results were seen in A549 cells. Our results suggest that δ ENaC is co-expressed with α, β, and γ ENaC proteins in human lung epithelial cells.

3.1.2. Co-immunoprecipitation of α and γ ENaC with δ ENaC in H441 cells. Co-expression of δ ENaC with α, β, and γ ENaC indicates that these four ENaC subunits may associate with each other to form channel complexes. To test this hypothesis, we first detected native δ ENaC protein expression in H441 cells. δ, α, and γ ENaC proteins were detected as 85~90 Kb for δ and α ENaC, respectively, and 150 Kb for γ ENaC. γ ENaC was found to co-immunoprecipitate with δ and α ENaC (Ji *et al.*, 2006). Specificity was demonstrated by Western blots with anti-γ ENaC following pretreatment of the anti-γ ENaC antibody with excess neutralizing peptide (Ji *et al.*, 2006). In addition, δ ENaC also precipitated with α ENaC subunit in H441 cells and in COS-7 cells following transiently transfection of hemagglutinin (HA)-tagged δ ENaC and α ENaC (Ji *et al.*, 2006).

3.1.3. Identification of a novel splicing variant for δ ENaC. We recently cloned a novel variant, namely, δ2 ENaC. δ2 ENaC encodes a full-length proteins comprised of 802 amino acid residues. In comparison, the aforementioned δ ENaC, termed δ1 ENaC here, encodes 638 amino acid residues (Ji *et al.*, 2012). Two genetic variants of δ ENaC were analyzed in human alveolar epithelial cells. We found in both alveolar type I and II cells, δ2 ENaC is expressed at a lower level than δ1 ENaC (Zhao *et al.*, 2012). In some cases, δ1 and δ2 were present in the same alveolar cells. In addition, δ1 ENaC was also present in pulmonary leukocytes, in which other ENaC subunits and amiloride-sensitive

channels have been detected (Bubien *et al.*, 2001).

3.2 δ ENaC confers the properties of αβγ ENaC channels

Native amiloride-sensitive Na^+ channels exhibit a variety of biophysical properties, including variable sensitivity to amiloride, different ion selectivity, and diverse unitary conductances. The molecular basis of these differences has not been elucidated. We tested the hypothesis that co-expression of δ ENaC underlies the multiplicity of amiloride-sensitive Na^+ conductances in epithelial cells.

3.2.1. Cation permeability. In this sets of experiments, we tested the hypothesis that co-expression of δ ENaC will alter the ion selectivity of αβγ channel. We found that the inward amiloride-sensitive Na^+ current was greater than that carried by Li^+ ions. Much less inward and relative greater outward currents were detected when K^+, Cs^+, Ca^{2+}, and Mg^{2+} were used as charge carriers. Meanwhile, the reversal potential shifted leftward from depolarization voltages (10 to 20 mV) by approximately 50 to 150 mV. Additionally, the resting membrane potentials, which were generally above zero mV under current clamp configuration in oocytes perfused with Na^+ (or Li^+), showed hyperpolarization to a variable extent (Ji *et al.*, 2004).

To calculate the permeability ratios between Na^+ and the other cations, amiloride-sensitive current-voltage curves were fitted with the Goldman-Hodgkin-Katz current equation as described previously (Ji *et al.*, 2001). The P_X/P_{Na} ratios of Na^+ /Li^+ /K^+ /Cs^+ /Ca^{2+} /Mg^{2+} were 1/**0.6**/0.07/0.2/0.26/0.4 for δβγ ENaC. However, they were 1/**1.2**/0.02/0.29/0.31/0.21 for αβγ-ENaC and 1/**0.88**/0.02/0.14/0.23/0.14 for δαβγ hENaC,

respectively. Our results of wild type αβγ and δβγ ENaC are consistent with previously published observations (Canessa *et al.*, 1994; Waldmann *et al.*, 1995; Ji & Benos, 2004). In particular, the normalized permeability to Li^+ (P_{Na} is 1.0) for δαβγ ENaC was 0.88, which was distinguishable from those of αβγ (1.2) and δβγ ENaC (0.6). Significant differences in normalized permeabilities to the other monovalent and divalent cations was not observed between heterologously expressed αβγ, δβγ, and δαβγ ENaC channels.

3.2.2. Amiloride sensitivity. The K_i of amiloride for δβγ ENaC is in the micromolar range (vs <100 nM for αβγ ENaC). Amiloride blocking of δβγ ENaC is much more voltage-dependent compared to αβγ channel (Ji & Benos, 2004). To determine amiloride sensitivity of δαβγ ENaC, we perfused oocytes with solutions containing 1nM, 10nM, 100nM, 1μM, 10μM, 100μM, and 1mM amiloride at holding potentials ranging from -120 mV to +80 mV. We observed that the dose-response curves shifted rightward at depolarized potentials. The K_i of amiloride at -120 mV was 920 ± 185 nM, and 13,746 ± 2805 nM at +80mV, respectively, which significantly differ from those of αβγ ENaC ($P < 0.05$) (Ji *et al.*, 2004).

To further investigate the voltage dependence of amiloride inhibition for δαβγ human ENaC channel, the retrieved values for K_i^{amil} were plotted against the membrane potentials (Ji *et al.*, 2004; Ji *et al.*, 2006). The more depolarizing the membrane potential, the greater the value of K_i^{amil}. As we have previously described for αβγ and δβγ ENaC, positively charged amiloride interacts with ENaC in a voltage-dependent manner (Ji & Benos, 2004). The K_i of amiloride at 0 mV estimated by fitting the voltage-

dependent plot with the Woodhill equation was 3.79 ± 0.2μM for δαβγ ENaC, whereas it was 13.1 μM and 0.33 μM for δβγ and αβγ ENaC, respectively (Ji *et al.*, 2004). The voltage sensitive fractional distance for amiloride was 0.41 (Ji *et al.*, 2004). In comparison, it was 0.34 for αβγ ENaC and 0.48 for δβγ ENaC, respectively (Ji *et al.*, 2004; Ji *et al.*, 2006).

3.2.3. Unitary conductance. Because the ion permeability ratio (P_{Na}/P_{Li}) and apparent equivalent dissociation constant of amiloride for the δαβγ ENaC channel are the arithmetic mean of those of αβγ and δβγ ENaC, the question arose whether oocytes injected with δαβγ ENaC subunits express two separate populations of ENaC, that is, αβγ and δβγ ENaC channels, or one population of δαβγ channels with novel biophysical characteristics. To address this question, on-cell patches were used to measure single channel conductances (Ji *et al.*, 2004; Ji *et al.*, 2006). Only one unitary Na^+ or Li^+ current level was observed and the corresponding slope conductances, respectively, were 8 ± 0.2 pS for Na^+ and 7.5 ± 0.1 pS for Li^+ ions. No amiloride-sensitive sub-conductance was observed (Ji *et al.*, 2004).

3.2.4. Gating kinetics. We measured the mean open time (MOT) and mean closed time (MCT) for δαβγ-ENaC (Ji *et al.*, 2006). We described that the MOT and MCT for δαβγ ENaC channels were significantly less than the corresponding values for αβγ and δβγ ENaC channels. The MOT values for αβγ and δβγ ENaC were greater than that of δαβγ ENaC ($P < 0.05$). In addition, the MCT values of αβγ ENaC was almost 10-fold of that for δαβγ ENaC ($P < 0.05$).

3.2.5. Proton activation. We found that $\delta\beta\gamma$, but not $\alpha\beta\gamma$ ENaC was activated by extracellular protons (Ji & Benos, 2004). To test the pH sensitivity of $\delta\alpha\beta\gamma$ ENaC, oocytes were perfused with bath solutions with neutral or acidic pH. Similar to the $\delta\beta\gamma$ ENaC channel expressed in oocytes, the inward current of $\delta\alpha\beta\gamma$ ENaC was activated by extraoocyte acidic pH in a concentration-dependent pattern (Ji *et al.*, 2006). The pH value required for half activation of the maximal pH-activated current level (EC_{50}) was 6.5 ± 0.1 (Ji *et al.*, 2004). This differs from pH 6.0 for $\delta\beta\gamma$ ENaC (Ji & Benos, 2004).

3.2.6. Self-inhibition. Self-inhibition by extracellular Na^+ ions is a biophysical hallmark of the ENaC channels (Garty & Palmer, 1997). To characterize this inherent biophysical property, the self-inhibition time of Na^+ for $\delta\alpha\beta\gamma$ ENaC was examined (Ji *et al.*, 2006). To calculate self-inhibition time, the currents at -60 mV were digitized while switching bath solutions from low Na^+ ND96 medium (1 mM Na^+ ions) to ND-96 (96 mM Na^+ ions) medium. The current fraction from the time point for the first time to switch bath solution (from 1 mM to 100 mM) to the peak of current (τ_a) and from the peak of current to the time point for the second time to switch bath solution (from 100 mM to 1 mM, τ_{si}) was fitted with the first-order exponential function for estimating τ_a (activation time) and τ_{si} (inactivation time), respectively (Ji *et al.*, 2006).

Our data shows that the inward current reaches its peak in less than 1 s followed by a run-down in the presence of constant external Na^+ level. The self-inhibition time (τ_{si}) for $\delta\alpha\beta\gamma$ ENaC was $3,427 \pm 217$ ms, which was significantly greater than that of $\alpha\beta\gamma$ ENaC ($2,584 \pm 72$ ms, $P < 0.05$) and but less than that of $\delta\beta\gamma$-ENaC ($8,626 \pm 1,541$ ms, $P < 0.01$). In contrast, the activation (τ_a) was not changed significantly. The $\alpha\beta\gamma$ ENaC

current displayed a steep run-down (45 % of the peak current in 12.5s) while the δβγ ENaC current level decreased to a less extent (12% of peak current in 12.5s) (Ji *et al.*, 2004). These results are consistent with measurements of rat and mouse αβγ ENaC expressed in oocytes (Chraibi & Horisberger, 2002; Sheng *et al.*, 2004). Therefore, the corresponding ratio of the peak and sustained currents was much less for αβγ ENAC compared with those of δβγ and δαβγ ENaC ($P < 0.01$).

3.2.7. Dependence of P_{Na}/P_{Li} ratio and unitary Na^+ conductance on injected cRNA concentrations. To determine the expression level of δ ENaC needed to confer the biophysical features of αβγ ENaC, we measured the P_{Li}/P_{Na} ratios and unitary Na^+ conductance in oocytes co-injected various ratios of δ and αβγ ENaC cRNAs (Ji *et al.*, 2006). The P_{Li}/P_{Na} ratio in oocytes co-injected with an equivalent concentration (1δ:1α) of δ and α ENaC cRNAs was significantly lower when compared to that of αβγ ENaC (0.7 vs 2.0, $P < 0.05$). Even with the cRNA ratio of 1δ:10α the relative Li^+ permeability reduced markedly. Meanwhile, the unitary Na^+ conductance increased in 1/3 of patches in oocytes expressing 1δ:10α ENaC. A further increase (10δ:1α) in the δ subunit cRNA co-injected elevated the conductance closing to the level of δβγ ENaC (Ji *et al.*, 2006).

In toto, reverse transcription PCR revealed that δ ENaC is co-expressed with αβγ subunits in several cultured human epithelial cells, including lung epithelial cells (H441 and A549), pancreatic cells (CFPAC), and colonic epithelial cells (Caco-2). Indirect immunofluorescence microscopy revealed δ ENaC is co-expressed with α, β, and γ ENaC in H441 cells at the protein level. The biophysical and pharmacological features between classical αβγ and δαβγ channels are different. We, therefore, conclude that δ

ENaC forms multimeric channels with $\alpha\beta\gamma$ subunits with novel biophysical features, thereby accounting at least in part, for the observed heterogeneity of biophysical properties of native epithelial Na^+ channels (Ji *et al.*, 2006).

3.3 Urokinase contributes to fluid homeostasis in pulmonary system

Concurrent existence of lung oedema and significant depressed fibrinolytic activity in oedematous lung injury indicates a link between the uPA/plasmin system and transepithelial fluid movement (Idell *et al.*, 1992a; Barazzone *et al.*, 1996; Sebag *et al.*, 2011; Tucker & Idell, 2013). We reported that plasminogen activator inhibitor (PAI-1) altered ENaC activity previously (Lazrak *et al.*, 2009). We also demonstrated that trypsin cleaved ENaC *in vitro* (Jovov *et al.*, 2002). uPA is a major contributor to the pulmonary fibrinolytic activity. An overwhelmingly elevated PAI-1 level in the BAL lavage was supposed to eliminate uPA activity (Idell, 2003; Shetty *et al.*, 2008; Sapru *et al.*, 2010). However, in normal lungs, uPA is readily detectable (Shetty *et al.*, 2008; Ji *et al.*, 2015). We thus hypothesize that uPA regulates transalveolar fluid clearance *in vivo*. To test this hypothesis, we utilized a mouse colony with deficient *uPA* gene, and the controls were wild type mice with the same genetic background. Furthermore, the underlying mechanisms were explored in primary cell cultures.

3.3.1. Characterization of ENaC activity in *uPA* knockout cells. Benzamil is a specific and potent inhibitor of ENaC activity (Kleyman *et al.*, 1999). We examined dose-effect relationship of benzamil in mouse tracheal epithelial (MTE) monolayer cells. Our results suggest that the level of basal short-circuit current (Isc) in WT cells is approximately four fold that in *uPA* knockout preparations. The Isc values were inhibited

by increasing the administered benzamil from 10 nM to 100 μM (Chen *et al.*, 2014). However, the *Ki* values for WT and *uPA*$^{-/-}$ cells do not differ significantly.

3.3.2. Reduction of ENaC activity in uPA-deficient MTE cells. Inflammation and suppressed uPA activity are known to co-exist in injured lungs (Idell *et al.*, 1992a; Barazzone *et al.*, 1996; Sebag *et al.*, 2011; Tucker & Idell, 2013). Based on the marked difference in ENaC activity between WT and *uPA*$^{-/-}$ cells, we postulated that uPA regulates ENaC activity in the airway epithelium. To test this hypothesis, we measured ENaC function in MTE monolayer cells collected from both WT and *uPA*$^{-/-}$ mice. MTE cells from age- and gender-matched mice were cultured at the air-liquid interface as described (Chen *et al.*, 2009). We found that basal activity in *uPA*$^{-/-}$ cells was reduced compared to that in WT controls. Amiloride, a widely used inhibitor of ENaC activity, reduced the predominant fraction in both WT and *uPA*$^{-/-}$ cells. In sharp contrast, the transepithelial resistance did not show any difference between these two groups, though amiloride increased the value slightly (Chen *et al.*, 2014). *uPA* deficiency caused a reduction of ~40 % in ENaC function (Chen *et al.*, 2014).

ENaC activity depends upon its phosphorylation by the cAMP/PKA signaling pathway. We therefore examined the effects of uPA on cAMP-activated ENaC activity. Cystic fibrosis transmembrane conductance regulator (CFTR) is also a target of the cAMP/PKA signaling pathway and functionally inter-regulates ENaC. CFTRinh-172 was used to eliminate CFTR function. Similar to the basal ENaC activity, a significant reduction in the cAMP-elevated ENaC activity was observed in *uPA*$^{-/-}$ cells (Chen *et al.*, 2014).

3.3.3. *uPA* deficiency down-regulates ENaC activity in permeabilized cells. Na^+ ion flow through ENaC channel pore is driven by both Na^+ ion gradient across the apical plasma membrane and Na^+/K^+-ATPase at the basolateral membrane. To measure ENaC activity, Na^+/K^+-ATPase was eliminated functionally in the basolateral membrane-permeabilized cells. In addition, electrogenic Cl^- flow via CFTR was completely blocked by symmetrical Cl^- concentration across the apical membrane. Under these conditions, we reevaluated ENaC activity with a physiological Na^+ ion gradient (Chen *et al.*, 2014). The rate of Na^+ influx through ENaC shows a significant decrease in *uPA*$^{-/-}$ cells. These data, combined with those from intact monolayer cells, support the concept that ENaC activity in MTE cells is down-regulated in the absence of uPA.

We next asked whether *uPA* knockout would affect Na^+/K^+-ATPase and indirectly down-regulate ENaC by eliminating the transepithelial Na^+ ion gradient. To answer this question, we compared Na^+/K^+-ATPase activity between WT and *uPA*$^{-/-}$ cells following apical membrane permeabilization (Chen *et al.*, 2014). Ouabain-inhibitable Isc fraction was approximately 50% that of WT cells. Clearly, depression of the driving force for ENaC results in reduced ENaC activity in *uPA*-deficient cells.

3.3.4. Phosphorylation of ERK1/2 and Akt by uPA. ERK1/2 and Akt are downstream components of the uPA/uPAR signaling pathway (Smith & Marshall, 2010). Furthermore, ENaC has been confirmed to be regulated by both phosphorylated ERK1/2 and Akt (Arteaga & Canessa, 2005; Lee *et al.*, 2007; Lazrak *et al.*, 2012). We reasoned that *uPA* deficiency regulated ENaC activity via modification of ERK1/2 and Akt phosphorylation (Figure 6). The first set of immunoblot assays was carried out with

lung tissues. A significant elevation in the ratio of phosphorylated versus total proteins for ERK1/2 was seen in *uPA*$^{-/-}$ lysates (Chen *et al.*, 2014). However, alteration in the

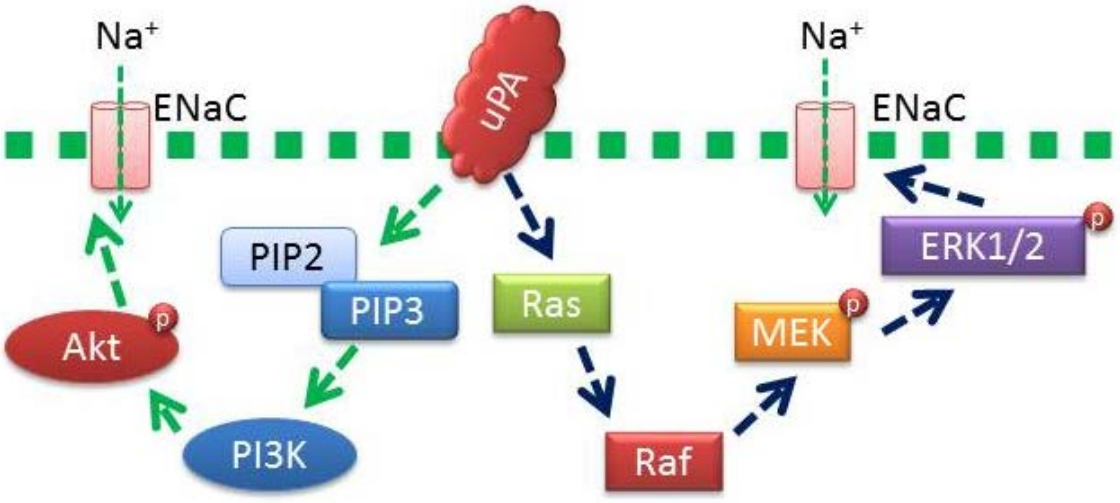

Figure 6. Diagram of the ERK1/2 and Akt as downstream molecules of the uPA. Signal pathway.

phosphorylation status of Akt was not observed neither in *uPA*$^{-/-}$ deficient MTE cells or lung homogenates. We then repeated these intriguing observations in cultured primary MTE cells. An incremental change in phosphorylated ERK1/2 proteins was found in *uPA*-deficient MTE cells. In striking contrast, a slight decline in phosphorylated Akt proteins was found. Is phosphorylation of ERK1/2 a mediator for the regulation of ENaC activity by uPA? To address this question, we knocked down ERK1/2 using specific siRNAs (Chen *et al.*, 2014). ENaC activity was restored up to approximately 90% of that in WT cells, indicating that uPA regulates ENaC via ERK1/2 phosphorylation.

3.3.5. Apoptosis is not involved in the reduction of ENaC activity. It has been documented that manipulation of *uPA* gene influences cellular apoptosis (Hildenbrand *et al.*, 2008; Prager *et al.*, 2009). Reduced ENaC activity could simply be due to abnormal cell survival. We addressed this issue by determining the expression

of caspase 8, an apoptotic marker in the WT and *uPA*$^{-/-}$ MTEs (Du *et al.*, 2006). Neither full-length nor cleaved caspase protein expression was augmented (Chen *et al.*, 2014). These results were supported by the transepithelial resistance measurement and demonstrate that the decreased ENaC activity in *uPA*$^{-/-}$ cells is not attributable to apoptotic transformation of the cells.

3.3.6. Proteolysis of ENaC by uPA. Urokinase belongs to the S1 family of serine proteases. The active triad is composed of histidine, aspartic acid, and serine residues. Heterologously expressed human and murine ENaC proteins have been confirmed to be proteolytically modified by plasmin (Passero *et al.*, 2008; Haerteis *et al.*, 2012). We postulate that uPA cleaves ENaC under physiological conditions, and that *uPA* deficiency depresses proteolysis of ENaC. To characterize a new polyclonal antibody against the C-terminal peptide of rat γ ENaC, proteins in Western blots loaded with both total and plasma membrane proteins from cells expressing mouse γ ENaC served as positive controls. The construct was tagged at the N-terminal with FLAG@ (trademark) epitope that can be specifically recognized by a monoclonal antibody against FLAG epitope. There are two specific bands (95 and 86 kDa) with anti-FLAG antibody, which was loaded with total proteins of cells expressing mouse γ ENaC with FLAG epitope. Similarly, the polyclonal ENaC antibody raised with the C-terminal peptide of rat γ ENaC recognized the same signals, which were loaded with total and plasma membrane protein, respectively. Importantly, this polyclonal antibody detected a cleaved C-terminal fragment with a size of approximately 74 kDa in wild type mouse lung tissues. Furthermore, we quantitated the cleavage of γ ENaC in *uPA* deficient

lungs using β-actin as a loading control (Chen *et al.*, 2014). Indeed, catalysis of γ ENaC was significantly reduced in the lungs of *uPA* disrupted mice.

3.3.7. Contribution of uPA to airway luminal fluid homeostasis. Homeostasis of respiratory luminal fluid is mainly regulated by ENaC (Mall *et al.*, 2008; Mall *et al.*, 2010; Lazrak *et al.*, 2011). We postulated that uPA-mediated ENaC activity in the airway epithelial cells may affect fluid re-absorption. To test this hypothesis, we measured fluid height at the apical surface of MTE (mouse tracheal epithelial) cultures using a well-characterized visualization approach (Tarran *et al.*, 2005; Hobbs *et al.*, 2013). We demonstrated that the depth of apical fluid above the *uPA*-deficient cells was much greater than that of WT controls ($P < 0.05$) (Chen *et al.*, 2014).

In summary, this set of studies provides novel evidence that uPA regulates ENaC activity via multifaceted mechanisms that relate to clearance of airway fluids in injured lungs. uPA exerts its effects on proteolysis of ENaC, regulation of Na^+/K^+-ATPase, and modification of ERK1/2 signaling. This work links alterations in the expression of uPA activity to altered ENaC functionality in injured lungs.

3.4 Urokinase plasminogen activator proteolytically cleaves γ ENaC subunits

There are at least four ENaC subunits (α, β, δ, γ) expressed in human respiratory epithelial cells. The question raised from above *in vivo* studies is what ENaC subunit is catalyzed by urokinase? To date, all of three subunits have been reported to be proteolytically cleaved, in particular α and γ ENaC proteins (Andreasen *et al.*, 2006; Planes & Caughey, 2007; Kleyman *et al.*, 2009). δ ENaC is not believed to be cleaved (Haerteis *et al.*, 2009; Giraldez *et al.*, 2012; Ji *et al.*, 2012). Our immunoblotting assay

suggests that at least fragments of native γ ENaC proteins in *uPA* deficient cells are altered (Chen *et al.*, 2014). To further identify the target subunit for uPA, we incubated *Xenopus* oocytes heterologously expressing various combinations of human αβγ ENaC subunits with two-chain uPA (tcuPA). Single chain uPA proteins were generally cleaved to form tcuPA with catalytic activity under physiological conditions. The cleavage of ENaC proteins was detected by combining functional analysis of ion channel activity with immunoblotting assays of catalyzed peptides.

3.4.1. γ ENaC is cleaved by uPA. To identify what subunits are cleaved by tcuPA, a well-established measurement of amiloride-sensitive sodium ion flow was applied (Ji *et al.*, 1998a; Ji *et al.*, 1998b, 1999; Ji *et al.*, 2000; Ji *et al.*, 2001; Ji *et al.*, 2002a; Ji *et al.*, 2002b). We expressed α alone, α + β, and α + γ in oocytes. tcuPA slightly stimulated current level in cells expressing α ENaC alone ($P > 0.05$). The change in cells co-expressing α + β ENaC subunits was not significant. In sharp contrast, the activity of channels composed of α + γ ENaC subunits was increased approximately three-fold ($P < 0.05$). These results indicate that the γ subunit could be a target for tcuPA.

3.4.2. Identification of cleavage regions in ENaC. As proposed and confirmed by several groups, there are three putative cleavage domains (Rossier, 2004; Planes & Caughey, 2007; Kleyman *et al.*, 2009; Rossier & Stutts, 2009). To narrow down the search range for uPA cleavage sites, we constructed three deletion mutants for both α (αΔ131-138, αΔ178-193, and αΔ410-422) and γ ENaC subunits (γΔ131-138, γΔ178-193, and γΔ410-422), and expressed them in oocytes. We reasoned that removal of tcuPA

cleavage sites from these ENaC subunits, channel activity associated with these cleavage site-missing mutants should not be altered by tcuPA. Intriguingly, four mutants, one of α ENaC and all three deletion mutants of γ ENaC subunit did not respond to tcuPA (Ji *et al.*, 2015). Because the current levels between each construct vary before application of uPA, we thus computed fold increased in the ENaC activity, suggesting that uPA-specific cleavage motif may be located within these four deleted ectodomains.

We then constructed V5 (C-terminal) and HA (N-terminal) tagged α ($^{HA}\alpha^{V5}$) and γ ENaC ($^{HA}\gamma^{V5}$) to examine tcuPA-mediated proteolysis combining biotinylation and Western blots. What we observed is that three bands of α ENaC were recognized by anti-V5 monoclonal antibody. One small fragment at 25 kDa in addition to a full-length signal was identified by anti-HA antibody (Ji *et al.*, 2015). Furthermore, three small bands could be visualized on 16.5% Tris-Tricine gels by anti-HA antibody. The same signal patterns of α ENaC were found in the absence and presence of tcuPA, either with anti-carboxyl terminus (-COOH) or anti-amino terminus (-NH2) antibody. These results exclude the cleavage of α ENaC proteins by tcuPA, further substantiating the functional analysis.

In strict contrast to α ENaC, two peptides of γ ENaC were visualized by anti-V5 antibody for full-length proteins (86 kDa) and endogenous furin-cleaved C-terminal fragments (70 kDa) in the absence of tcuPA (Ji *et al.*, 2015). By comparison, in the presence of tcuPA, C-terminal fragments with a smaller size (65 kDa) than that of furin-cut fragments along with the full-length proteins were seen. Strikingly different from anti-V5 antibody-recognized signals, proteins detected by anti-HA monoclonal antibody

displayed a similar pattern, either on 7.5 % SDS-PAGE gels or 16.5% Tris-Tricine gels. The same pattern for ENaC expression was found between controls and tcuPA-treated groups, indicating that the furin sites may precede the cleavage domains for tcuPA. Thus, the subsequent Western blots were done with anti-V5 antibody to examine uPA-cleaved C-terminal peptides as well as full-length translations (Ji *et al.*, 2015).

3.4.3. An uPA substrate in γ ENaC. Several serine proteases, including prostasin (RKRK178), human neutrophil elastase (V182, V193), and plasmin (K189) trimmed the second consensus proteolysis motif (Rossier, 2004; Planes & Caughey, 2007; Kleyman *et al.*, 2009; Rossier & Stutts, 2009). It is conceivable that all these residues are targeted by tcuPA. This is at least the scenario for substrate-less specific plasmin to cleave human γ ENaC (Haerteis *et al.*, 2012). Indeed, the plasmin cleavage site composed of five amino acid residues for prostasin and one for murine plasmin (^{178}RKRK^{181} + K189), when substituted with alanine (termed γ5A, ^{178}AAAA^{181} + A189) was not stimulated by tcuPA even after 24 h (Ji *et al.*, 2015). Moreover, the tcuPA-cleaved band disappeared compared with that of wild type channels (Ji *et al.*, 2015).

A series of classic studies on the specificity of uPA substrates revealed a consensus cleavage motif, GR↓(S>N/K/R)(A>>S) from P2 to P2' (Ke *et al.*, 1997a; Ke *et al.*, 1997b). We further combined *in silico* prediction and immunoblotting assays to narrow down the cleavage site. Using the SitePrediction server (Verspurten *et al.*, 2009), only one hit was predicted: 177GR↓KR within the ectodomain of human γ ENaC with a specificity above 99%. In strict contrast, no specific cleavage sites in human γ ENaC were found for tPA with its cleavage motif, (F/Y/R)GR↓R(A/G) from P3 to P2' amino acid residues. In addition, there are no predicted cleavage sites in human α, β,

and δ ENaC proteins for uPA to meet the prediction criteria. Does uPA cut γ ENaC proteins into two fragments between Arg178 and Lys179? We validated this prediction combining mutagenesis, functional measurements, biotinylation, and immunoblotting assays. Neither γR178A nor γK179A could be activated by tcuPA in 24 h significantly (Ji *et al.*, 2015). We anticipated that the uPA-cleaved band of R178A and K179A should migrate slower than that wild type if any. Intriguingly, it is the case for K179M, and probably K179A but not R178A. This phenomenon is consistent with the functional data measured as amiloride-sensitive sodium currents (Ji *et al.*, 2015). Combined with the blot for the deletion mutant, we believe that amino acid residues from P2-P2' (^{177}GRKR^{180}) coordinately interact with uPA to serve as a catalytic triad. Of them, both R178 and K179 amino acid residues are critical for uPA-mediated proteolysis.

Combined with *in silico* prediction, mutagenesis, electrophysiological measurements, and immunoblotting assays, for the first time, we demonstrate human γ ENaC is a new substrate for uPA. Furthermore, we identified a specific motif with identical sequence to the proven substrate for uPA. These novel results provide molecular basis for the underlying mechanisms for uPA to activate ENaC. Genetic variance of the cleavage sites in γ ENaC may lead to *uPA*-deficient like dysfunctional fluid clearance in the airways and lungs.

3.5 Localization of "cutting edge" of urokinase to catalyze ENaC

3.5.1. uPA but not tPA activates ENaC. Fibrinolytic activity is depressed in injured organs (*e.g.* in acute lung injury and pleural effusion) (Bertozzi *et al.*, 1990; Idell *et al.*, 1991; Sisson *et al.*, 2002; Prabhakaran *et al.*, 2003; Sapru *et al.*, 2010). These organ injuries are characterized by fluid accumulation in the luminal cavities, where

ENaC is critical for fluid resolution (Matthay *et al.*, 2002; Matthay *et al.*, 2005; Eaton *et al.*, 2009; Ji *et al.*, 2012). Both uPA and tPA initiate fibrinolysis by converting plasminogen to plasmin. To examine the specificity of uPA on ENaC activity, we compared the effects of uPA and tPA (Ji *et al.*, 2015). tcuPA stimulated ENaC activity in a dose-dependent manner. A linear relationship was seen between tcuPA concentration above 5 μg/ml (100 nM) and ENaC currents (Ji *et al.*, 2015). Furthermore, we characterized the time course for the activation of ENaC function by tcuPA. ENaC activity was quickly elevated at 2 h, followed by a slow increment, finally reaching maximal activity at 8 h post-treatment. The ENaC currents subsequently declined slightly but were still significantly greater than the control ($P < 0.05$) at 24 h. The uPA enzyme activity was 80 and 20% of the initial level, at 8 and 24 h, respectively. Insufficient enzyme, altered endocytosis of channel proteins, and time-dependent expression of exogenous ENaC channels may contribute to the slight decline of current level after the 8 h time point.

Surprisingly, neither single-chain tPA (sctPA) nor two-chain tPA (tctPA) at a dose of 10 ug/ml altered ENaC activity (Ji *et al.*, 2015). Tenecteplase was tested next to determine whether exosite interactions contribute to a sharp difference in the effects of tPA and uPA on ENaC activity. Tenecteplase is a mutant variant (T103N/N117Q/K296A/ H297A/R298A/R299A) of tPA, which has higher than WT tPA fibrin specificity, and almost 2 orders of magnitude lower affinity for PAI-1 due to the elimination of positive charges in the 37-loop (57–59). However, neither sctPA nor tctPA nor tenecteplase in doses as high as 25 ug/ml affected ENaC activity (Ji *et al.*, 2015), whereas enzymatic amidolytic activity toward LMW substrates and plasminogen-

activating activity remained intact. Our study hereby adds a novel endogenous target to the uPA substrate pool.

3.5.2. Catalytic triad of uPA to cleave ENaC. The two polypeptide chains of an uPA molecule (amino-terminal fragment (ATF) and protease domain) are connected by a single disulfide bond between two cysteine residues. To evaluate the contribution of uPA catalytic and ATF domains to activation of ENaC, a catalytically inactive S195A (chymotrypsin numbering) tcuPA and three uPA domain-deletion mutants, ∆kringle (deletion of Kringle domain), ∆CPD (deletion of Connecting Peptide Domain), and ∆GFD (deletion of Growth Factor Domain) uPA, were compared with WT tcuPA. Oocytes expressing ENaC cRNA cultured in medium without uPA or its mutants were used as a negative control (Ji *et al.*, 2015). Whereas inactive S195A tcuPA did not elevate ENaC current, all three mutant variants, which include the catalytic domain and possess enzymatic activity, activated ENaC. Therefore, there is only minimal (if any) contribution of ATF to ENaC activation by uPA (Ji *et al.*, 2015).

To further confirm these intriguing observations and to exclude the bias associated with enzymatic activity of each preparation of wild type and mutated uPA, we repeated these experiments by incubating oocytes with both wild type and mutant tcuPA preparations that, except for the S195A mutant, have equivalent enzymatic activity (Ji *et al.*, 2015). Consistent with the above experiment, the S195A tcuPA (negative control for this set experiments) did not affect ENaC activity. These three domain-deletion mutants of uPA, namely, ∆kringle, ∆CPD, and ∆GFD, stimulated ENaC currents to an extent similar to WT tcuPA. These data demonstrate that the amino-terminal fragment is not

involved in the activation of ENaC by tcuPA. Moreover, the same level of enzymatic activity associated with both wild type and mutant tcuPA, instead of identical mass, determined the amplitude of ENaC currents. We pooled experimental paired data for WT and mutated uPA as well as tPA constructs to compute the Pearson correlation. A correlation co-efficient of 0.93 was derived with a P value of 3.5E-6 between tcuPA and ENaC activity (Ji *et al.*, 2015). In sharp contrast, tPA enzyme activity showed no correlation with ENaC function. These results suggest a possible correlation between activated ENaC current levels and uPA enzyme activity, demonstrating that S195 is required for uPA to cleave ENaC.

3.5.3. Structural interactions between catalytic sites of uPA and cleavage sites of γ ENaC. The cleavage sites in the γ ENaC (R178 and K179) are located between α1 and α2 domains of the finger, a hypervariate region. The confident docking of the uPA specific cleavage site into the enzyme active center of uPA substantiates their protein-protein interactions (Ji *et al.*, 2015). A network of hydrogen bonds within the catalytic triad of uPA was visualized (Figure 7). Importantly, hydrogen bonding pairs are detected between His57 (uPA) and Lys179/Arg180 (ENaC), and Ser195 (uPA) and Arg178/Lys179 (ENaC). Beside, Thr176 (ENaC) interacts with His99 (uPA). Arg178 (ENaC) protrudes down into a deep cavity and interacts with other residues in the bottom of the cavity. Proteolysis of ENaC by uPA could be divided into two steps: acylation and deacylation (Neitzel, 2010). The Ser195 of uPA, together with His and Asp, serves as a nucleophilic “edge” to separate the Arg178 from Lys179 of γ ENaC, generating two fragments: the C-terminal peptide and the N-terminal peptide.

3.6 Urokinase augments opening channel density and opening time of channels

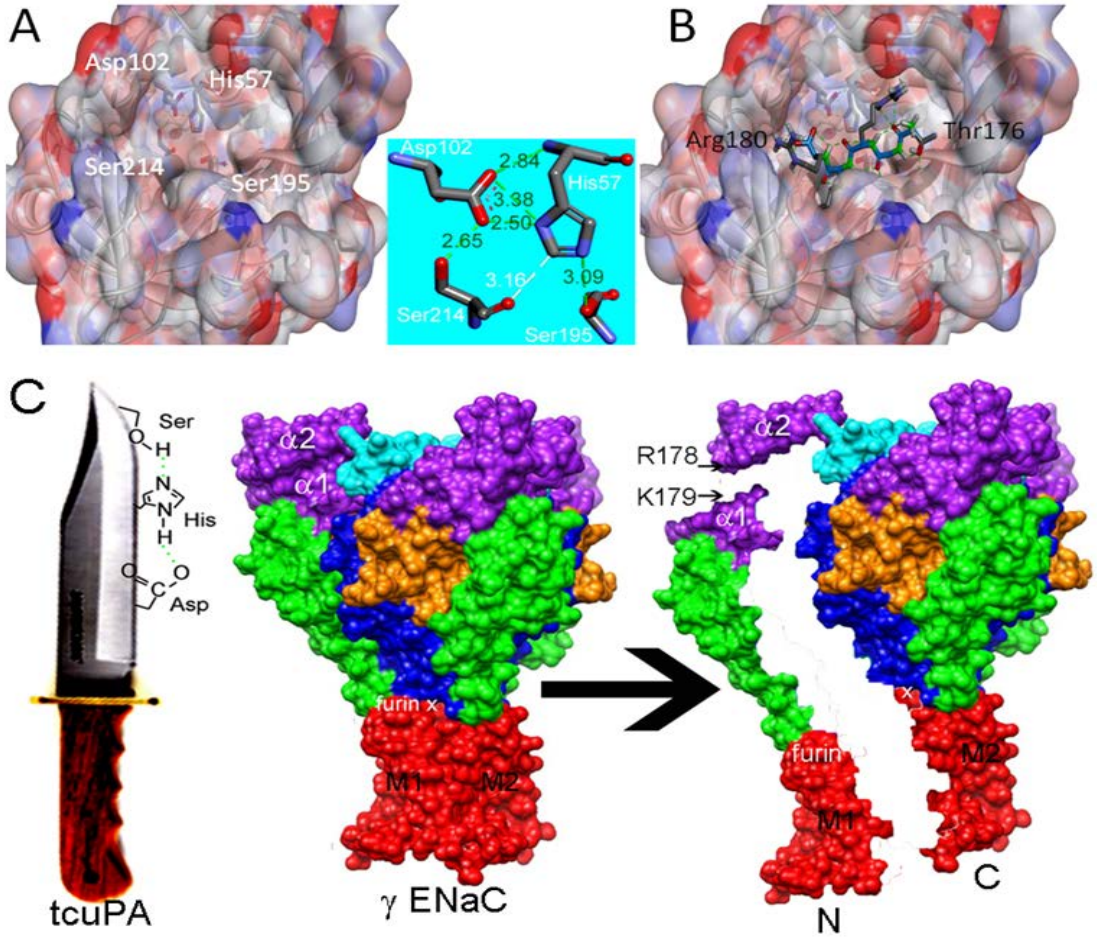

Figure 7. Structural interactions between uPA and human γ ENaC. *A*, *surface view* of the catalytic triad of uPA (Protein Data Bank code 1W12). The triad residues (Asp-102, His-57, and Ser-195) along with His-99 line the back of the enzyme active center. *Inset*, measures of hydrogen (*green* and *white dashed lines*) bonds among amino acid residues composed of the catalytic triad. *B*, docking of the cleavage site (P3–P2') of γ ENaC to the enzyme active pore of uPA. *C*, uPA-induced cleavage of the γ ENaC. Arg-178 and Lys-179 are located between the α1 and α2 domains. Domain coloration is as follows: transmembrane domains 1 and 2 (*TM1* and *TM2*) (*red*), wrist (*red*), palm (*blue*), knuckle (*cyan*), finger (*purple*), thumb (*green*), and β (*orange*). The three-dimensional uPA-cleaved sites from P3 to P2' in human □ ENaC (TGR ↓ KR) was generated by using "Tools>Build and Edit Protein" in Discovery Studio Visualizer version 4.0. Following removal of the ligand from uPA, docking of the cleavage site in ENaC to uPA was performed with Autodock Vina version 1.1.1 in a Pyrx (version 0.85) environment. The top-ranking pose with minimal energy in the docking results was selected and saved as a Protein Data Bank file. Final presentation was accomplished with Discovery Studio Visualizer version 4.0 by inserting the selected docking pose of the cleavage sites into the catalytic triad of uPA protein. The docking structure of uPA and cleavage site was further energy-minimized by "clean geometry." The uPA-ENaC interactions between the enzymatic domain and cleavage sites were visualized by a "non-bond interaction monitor" for a ligand-receptor mode. Adapted

3.6.1. uPA strengthens the open conformation of ENaC. A two-state model (closed-open) has been proposed to analyze the gating kinetics of ENaC channels (Chraibi & Horisberger, 2002). We postulated that tcuPA opens closed channels and facilitates maintenance of activated ENaC in the open state. To analyze this, the gating kinetics is computed by measuring self-inhibition of external Na^+ ions (Ji *et al.*, 2015). In addition to stable channel activity (reflected by sustained current level), the maximal channel activity (measured as peak current) was significantly greater than in control cells. The ratio of sustained over maximal current levels is approximately 0.5 for ENaC channels in control cells, which is consistent with previous observations (Sheng *et al.*, 2004; Sheng *et al.*, 2007; Molina *et al.*, 2011). By comparison, our results showed that the value was close to 1.0 following exposure to tcuPA. These studies suggest that self-inhibition is diminished by tcuPA. There are two components of self-inhibition: a fast phase followed by a slow phase (Garty & Benos, 1988; Ji *et al.*, 2015). The rate of activation process after incubation with tcuPA was almost an order of magnitude faster than that for untreated cells (1.17 and 11.9 s^{-1} for control and tcuPA treatment, respectively). Moreover, treatment with tcuPA completely eliminated inactivation (inactivation rate was reduced by tcuPA from 0.56 s^{-1} to 0.0 s^{-1}). In addition, even with switched gating rates between control and tcuPA-treated cells, the simulated maximal current level at the full open state for controls was still much lower than the sustained current magnitude of tcuPA-challenged cells. These observations could not simply be explained by full opening of activated channels in untreated cells. On the other hand, irreversibility of the effect of tcuPA on ENaC gates most likely reflects cleavage of ENaC by tcuPA resulting in transition to the “open” conformation of the channel.

3.6.2. uPA activates "silent" channels. Channel activity recorded in whole-cell mode is the product of single channel activity and unitary conductance. The latter was not altered during self-inhibition, as has been demonstrated by self-inhibition mutations (Sheng *et al.*, 2004; Molina *et al.*, 2011). Single channel activity is the product of open probability and electrically detectable channel density. The simulation leads us to ask whether there is a potential increment in functional channel density. The functional channel density was computed as we described recently (Ji *et al.*, 2015). Our calculation found that the channel number that could be detected per unit area was 410 channels /μm^2 post uPA exposure. It is five-fold greater than that in control cells (82 channels/μm^2). It appears that uPA increases functional channel density at the plasma membrane. This is supported by studies of other serine proteases (Caldwell *et al.*, 2004, 2005; Diakov *et al.*, 2008).

3.6.3. uPA optimally increases opening time. MTSET is a thiol-modifying reagent that activates $\alpha\beta$S520Cγ channels almost completely as evidenced by an open probability of nearly 1.0 (Goldfarb *et al.*, 2006). If uPA activates ENaC activity via an increment in opening time, with a mechanism similar to that mediated by MTSET, then uPA should not alter ENaC whole-cell currents in MTSET-pretreated cells expressing $\alpha\beta$S520Cγ channels. Our results indicate that while MTSET does increase channel activity in untreated cells to a level similar to that in uPA-incubated cells (Ji *et al.*, 2015), it does not affect uPA-activated ENaC activity. These observations provide direct evidence for uPA maintenance of ENaC channels in the fully open state, with a resultant effect equivalent to that of MTSET.

3.7 Proteolysis is the mechanism to elevate ENaC activity to the utmost level vs self-inhibition releasing agents

Cpt-cAMP, as a cell permeable specific PKA activator has long been used for studying epithelial Na^+ channels. Chraibi and colleagues found that the compound specifically activated guinea pig but not rat ENaC in oocytes (Chraibi *et al.*, 2001). Furthermore, a key responsive domain in guinea pig α subunit (Ile481) was identified (Renauld *et al.*, 2008). Human ENaC responded to cpt-cAMP in a dose-dependent, time-independent, and reversible manner. In addition to these heterologous channels, amiloride-sensitive, cpt-cAMP activated cation channels were also reported in human Clara cells (H441) and human lymphocytes in a similar manner (Bubien *et al.*, 1996; Bubien *et al.*, 1998; Bubien *et al.*, 2001; Chen *et al.*, 2009). To date, the interpretation for the acute activation of both native and heterologous human ENaC activity by cpt-cAMP is still limited to the mediation of the cAMP/PKA pathway. A number of critical amino acid residues are involved in governing self-inhibition. External sodium self-inhibition is an intrinsic feature of ENaC. A rapidly increase in extracellular sodium ions to a physiological concentration (150 mM for mammals and 100 mM for amphibians) generates a maximal peak current in seconds, and then the permeability of ENaC to Na^+ ions is gradually reduced to a relatively stable level with a current level of approximately half of the maximal value. This phenomenon is called extracellular sodium self-inhibition of ENaC activity. It differs from the down-regulation of ENaC activity by slowly accumulating intracellular Na^+ content in a feedback manner. External Na^+ self-inhibition is a crucial mechanism to limit overwhelming salt absorption to prevent a quick raise in epithelial cell volume and blood pressure. Sheng and co-

workers identified the cysteine and histidine residues in α and γ subunits were critical (Sheng *et al.*, 2002; Sheng *et al.*, 2007). Very recently, this group provided strong evidence that αGly481 and γMet438 resided in the thumb domain were functional determinants of self-inhibition (Maarouf *et al.*, 2009). In addition to the relief of self-inhibition, the external ligand-like compounds activated ENaC channels analog to serine proteases (Planes & Caughey, 2007; Kleyman *et al.*, 2009; Rossier & Stutts, 2009).

3.7.1. cpt-cAMP cannot activate cleaved ENaC by fibrinolysin. We hypothesize that uPA and cpt-cAMP activate ENaC with variant mechanisms and to a different extent. We tested the effects of cpt-cAMP on fully opened channels in cells exposed to protease-plasmin (Passero *et al.*, 2008; Svenningsen *et al.*, 2009a; Svenningsen *et al.*, 2009b). Our previous studies showed that external cpt-cAMP stimulated human, but not rat and murine, $\alpha\beta\gamma$ ENaC in a dose-dependent and external sodium concentration-dependent fashion (Molina *et al.*, 2011). ENaC mutations that abolished self-inhibition ($\beta\Delta$V348 and γH233R) almost completely eliminated cpt-cAMP mediated activation. In contrast, mutations that both enhanced self-inhibition and elevated cpt-cAMP sensitivity increased the stimulating effects of the compound. Our above data confirmed that cpt-cAMP acts as a ligand to regulate heterologous ENaC by relieving self-inhibition. Edelheit et al studied alanine mutations in 17 conserved charged residues of ENaC and found that these residues are involved in conformational changes that lead to channel constriction and to the sodium self-inhibition response upon sodium ion flooding (Edelheit *et al.*, 2014). Similarly, our recent data showed that elimination of self-inhibition of $\alpha\beta\gamma$ ENaC may be a novel mechanism for CPT-cGMP to stimulate salt reabsorption in the human epithelium (Han *et al.*, 2011).

3.7.2. Cleavage abolishes cpt-cAMP-mediated ENaC activation in human lung epithelial cells. To corroborate the findings in oocytes, we evaluated the effects of cpt-cAMP on native ENaC in human lung epithelial cells (H441 monolayers), in which biochemically and physiologically detectable ENaCs were evoked by cpt-cAMP (Chen *et al.*, 2009). cpt-cAMP activated amiloride-inhibitable Isc levels by approximately 8% (Molina *et al.*, 2011), which was much less than that for cloned ENaC in oocytes (2 fold). It is possible that ENaC proteins in carcinomatous H441 cells probably have been cleaved by overexpressed proteases (McMahon & Kwaan, 2008; Shetty *et al.*, 2008). We thus incubated cells with protease inhibitors for 12 h. As anticipated, cpt-cAMP increased Isc level up to 2-fold in cells pretreated with protease inhibitors (Molina *et al.*, 2011).

3.7.3. CPT-cGMP ligand docking to different ENaC domains. In our previous experiment, we constructed mutants abolishing (βV348 and γH233R), or augmenting (αY458A and γM432G), ENaC self-inhibition (Han *et al.*, 2011; Molina *et al.*, 2011). The mutations eliminating self-inhibition resulted in a loss of response to CPT-cGMP, whereas those enhancing self-inhibition facilitated the stimulatory effects of this compound. Our analysis shows the potential binding sites for the CPT-cGMP ligand in ENaC domains that are crucial for self-inhibition. βV348 is located in the center of the palm region of the subunit, and γH233 is located in the vicinity of the putative binding site for protons. These domains potentially directly or allosterically interact with CPT-cGMP.

3.7.4. CPT-cGMP and self-inhibition. Human serum cGMP level is 6 nM and 3-time greater in human bronchioalveolar lavage (Arias-Diaz *et al.*, 1994). It appears that cGMP may serve as an autocrine and paracrine to regulate ENaC function. However, the effective dose for CPT-cGMP and CPT-cAMP to blunt self-inhibition is micromolar, suggesting an uncertain physiological role for cGMP and analogs. A large dose of cGMP compound (1 mg/kg, i.v.) was administered to pigs as reported by a pre-clinical trial (Sandera *et al.*, 2000), and numerous preclinical studies (from 100 mM to 2 mM) (Jain *et al.*, 1998; Kemp *et al.*, 2001; Chen *et al.*, 2008). It is therefore feasible to apply aerosolized nucleotides to mitigate oedematous lung injury. We have demonstrated that CPT-cGMP up-regulates ENaC via two mechanisms: release self-inhibition externally and activates ENaC through the cGMP/cGKII pathway intracellularly (Han *et al.*, 2011). Thus, these compounds could regulate sodium absorption via either or both mechanisms in a cell permeability-dependent manner. Administration of cAMP could be a potent pharmaceutical treatment for oedematous lung injury (Chen *et al.*, 2009), and cGMP may have similar potential. cGMP increased in murine and rat lungs both *in vivo* and *in vitro* following nitric oxide (NO) application (Hardiman *et al.*, 2004), and increased cGMP may augment the cGMP-sensitive pathway for lung fluid removal from alveolar sacs (Sakuma *et al.*, 2004). Our previous study demonstrated for the first time that PKGII is an ENaC activator in non-ciliated bronchial secretory cells (Nie *et al.*, 2009b). Accordingly, upregulation of the rate-limiting ENaCs in respiratory epithelial cells by specific PKGII activators may be a potent clinicopharmaceutical strategy for alleviating airspace flooding in fatal oedematous lung diseases. The observation of our previous study that specific moieties of 8-pCPT-cGMP are required for activating ENaC may

provide pivotal information for developing potential ENaC channel openers structurally related to 8-pCPT-cGMP, which would be extremely useful for treating diseases associated with lower ENaC function. We postulate that when the tight epithelial layer is damaged, for example, in injured lungs, even though the mixture of extracellular matrix proteins, including collagens, albumin, and fibrins, will seal the epithelial cell-free alveolar surface, the potency of ENaC stimulator will be limited significantly. Therefore, the integrity of the tight alveolar epithelium should be a key factor to be considered for the usage of ENaC agonists. The anticipated restore of alveolar fluid clearance may be seen at the earlier stage of ALI and lung oedema mainly caused by injured pulmonary vasculature or post regeneration of alveolar epithelium by stem cells/progenitors.

3.7.5. Specific self-inhibition domains differ from uPA cleavage sites. His(88) and Asp(516) of the γ subunit play a role in the Zn^{2+} regulating sodium self-inhibition mentioned above. Recent studies showed that palmitoylation of the γ subunit activates ENaC by increasing the open probability of the channels (Mukherjee *et al.*, 2014). ENaC mutants with the mutations γC33A, γC41A, or γC33A/C41A have significantly enhanced sodium self-inhibition and reduced open probability compared with wild type ENaCs, suggesting that ENaC palmitoylation is an important post-translational mechanism of channel regulation. Exon 11 within the human α, β, and γ ENaC genes encodes structurally homologous yet functionally diverse domains, and exon 11 in the α-subunit encodes a module that regulates channel gating (Chen *et al.*, 2014). In contrast to the other mutations, γL511Q largely eliminated the sodium self-inhibition response, reflecting a down-regulation of ENaC open probability by extracellular sodium (Chen *et al.*, 2013). γL511Q is a gain-of-function human ENaC

variant and it enhances ENaC activity by increasing channel open probability and dampens channel regulation by extracellular sodium and proteases (Chen *et al.*, 2013).

3.7.6. Self-Inhibition as an alternative approach to fibrinolysins. Divergent targeting subunits and critical domains indicate that self-inhibition releasing reagents and fibrinolysins can be used as potential therapeutic strategies complementarily. Distressed transapical sodium transport occurs in injured lungs, for example, acute lung injury (ALI) and acute respiratory distress syndrome (ARDS) (please see classical reviews (Matalon *et al.*, 2002; Matthay *et al.*, 2002; Berthiaume & Matthay, 2007; Eaton *et al.*, 2009; Matalon *et al.*, 2015)). Apical ENaC contributes to up to 70% of transepithelial sodium transport in mammalian lungs under physiological conditions. This critical process is sensitive to aspirated pollutants, allergens, pathogens, and bacterial endotoxins. In addition to increased leaking through alveolar microvascular endothelium (indirect ALI), lung oedema ususally results from reduced oedema fluid resolution via ENaC (direct ALI). ENaC is a promising target for developing new therapeutical strategies to alleviate lung oedema, at least for the phenotype of direct ALI (Giraldez *et al.*, 2013; Czikora *et al.*, 2014).

4. Theoretical Framework

4.1. How and in what respect the work has made a significant and coherent contribution to knowledge. It is widely accepted that apical ENaC is composed of αβγ three subunits, given the fact that mice with deficient α ENaC (*scnn1a* gene) died after birth (Hummler *et al.*, 1996; Hummler & Vallon, 2005). The current concept is that pulmonary α ENaC function is amplified by βγ counterparts. Based on these earlier observations, it has been assumed that the fourth ENaC, that is, δ ENaC may not have a role in human lungs. Of note, the *scnn1d* gene is a pseudogene in murine but expressed in humans. On the other hand, infants carrying "loss-of-function" genetic mutants of *scnn1a* did not have respiratory distress syndrome. One explanation is *scnn1a* may have unknown functions that cause death. An alternative possibility is that δ ENaC may compensate the salt transport function in *scnn1a* deficient infants. The contributions of δ ENaC has long puzzled ENaC researchers due to lack of animal models. Our publications systematically characterized the expression and function of δ ENaC in pulmonary epithelium with complimentary techniques and models. Our studies clearly demonstrate that δ ENaC is approximately expressed in alveolar epithelial cells and function in a way similar to α ENaC. Our results for the first time outline the role of δ ENaC in pulmonary epithelial cells and shift the current concept about the components of apical ENaC channels.

Albeit fibrinolysins have been applied to pulmonary diseases, their mechanisms remain obscure, in particular for urokinase and plasmin. Our innovative studies for the first time demonstrate: 1) urokinase deficiency reduced ENaC function via a reduction in

Na^+/K^+-ATPase, ERK1/2 phosphorylation, and cleavage of γ ENaC subunit *in vivo*; 2) urokinase but not tissue-type plasminogen activator (tPA) up regulates human ENaC function in a dose-, time- and catalytic activity-dependent manner; 3) urokinase proteolytically cleaves γ ENaC subunit (R178↓K179) into two fragments; 4) urokinase augments activation rate and eliminates "silent" channels; 5) plasmin stimulates ENaC in a way similar to urokinase; and 5) a nucleotide (cpt-cAMP and CPT-cGMP) activates ENaC by releasing external sodium inhibition, differing from aforementioned mechanisms for fibrinolysins.

4.2. Impact. Abnormal fluid regulation in the respiratory system is the major pathological characteristics of both "dry" and "wet" lungs. Dehydration of the airways and the airspaces is associated with cystic fibrosis, chronic obstructive pulmonary disease (COPD), and genetic diseases with gain-of-function mutants of ENaC (Boucher, 2007; Mall *et al.*, 2010; Zhao *et al.*, 2014; Mall, 2016). Pulmonary oedema is a life-threatening clinical disorder. Cardiogenic pulmonary oedema (hydrostatic oedema) is caused by cardiovascular diseases, in particular heart failure. Noncardiogenic oedema results from systemic or pulmonary infection, brain trauma (neurogenic), side-effects of medicines, and high altitude (HAPE). ENaC contributes to ~70 % of alveolar fluid clearance and re-absorption of airway surface fluid. Our studies shift the current concept of the pulmonary epithelial sodium transport pathway. Our data improve our understanding in the pathogenesis of pulmonary oedema, and our knowledge in the physiological functions and pathogenic role of fibrinolysin-regulated ENaC in pulmonary

oedema. Our novel results provide cellular and molecular basis for the use of fibrinolysins to oedematous lung diseases.

4.3. Methodologies. We combined state-of-the-art electrophysiological (the voltage clamping, Ussing chamber, and patch clamping assays), contemporary biochemical (biotinylation, immunoblotting, ELISA, and immunofluorescent scoping), molecular biological approaches (mutagenesis, RT-PCR, *in silico* prediction, and *in vitro* cRNA), preclinical tests (alveolar fluid clearance, ventilation, *in vivo* intratracheal instillation, and histology), and leading edge techniques of gene modification (knockout, shRNA knock down, transgenic) to study the pharmaceutical mechanisms of nucleotides and fibrinolysins-mediated regulation of ENaC activity. The genetically engineered animals were used for *in vivo* studies, human lungs for *ex vivo* and *in situ*, primary cultures for *in vitro*, and expression system (*Xenopus* oocyte) for advanced mechanistic studies.

5. Summary/Conclusions

In summary, our results for the first time demonstrate that 1) δ ENaC is crucial to maintain fluid homeostasis in the airways and the airspaces; 2) pulmonary fibrinolytic activity regulates fluid homeostasis by proteolytically cleaves apical located ENaC proteins. Our data explain the species differences in the *scnn1a* deficiency-associated respiratory distress syndrome between human and mice, and in the pharmaceutical

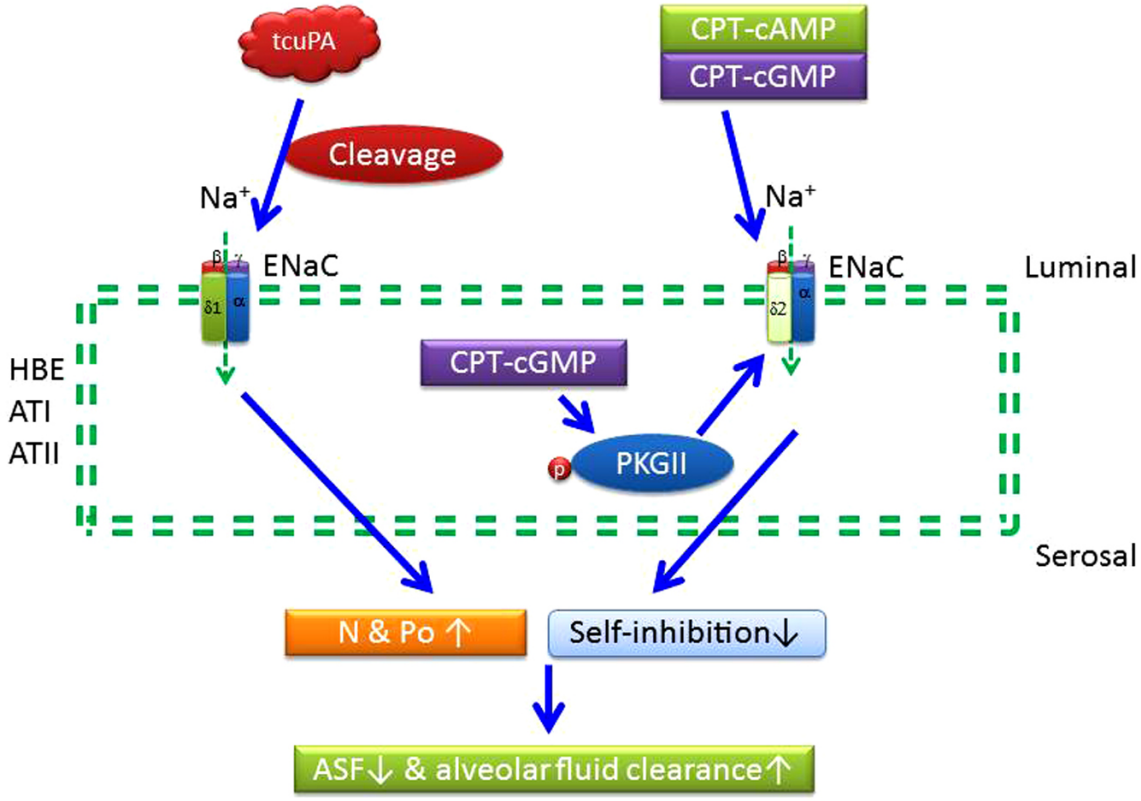

Figure 8. Graphical abstract to summarize key findings. tcuPA, two-chain urokinase plasminogen activator; PKGII, protein kinase G isoform 2; ENaC, epithelial sodium channels; HBE, human bronchial epithelial cells; ATI, alveolar type I cells; ATII, alveolar type II cells; N, ENaC channel density; Po, open probability; ASF, airway surface fluid.

efficiency and tissue dependence between tPA and uPA. In ENaC-expressing epithelial and mesothelial tissues, *e.g.*, the airways, lungs, pleural cavity, kidney, and distal colon,

it should be kept in mind that either endogenous or administered uPA may dehydrate the lumen through excessive activation of ENaC-mediated salt/fluid retention (Figure 8). For the first time, we demonstrate that cpt-cAMP and CPT-cGMP activate pulmonary ENaC by eliminating self-inhibition. Conclusively, our publications suggest that uPA, cpt-cAMP, and CPT-cGMP may be a novel generation of ENaC activators to mitigate lung oedema and other oedematous pulmonary diseases.

6. Contributions made by the candidate

By collaborating with a group of investigators on campus and worldwide, the first set of experiments was designed to characterize the expression and function of δ ENaC as well as a splicing variant in human lung epithelial cells (Ji *et al.*, 2006; Ji *et al.*, 2012; Zhao *et al.*, 2012). Furthermore, I found that δ ENaC conferred the biophysical and pharmacological properties of "classical" αβγ ENaC channels when four ENaC subunits are co-expressed in *Xenopus* oocytes heterologously (Ji *et al.*, 2006). These experiments were completed by collaborating with Drs. Zhao, Nie, Su, Han, Chang, Matalon, Kedar, Barbry, Smith, and Benos.

The second set of experiments was set out to examine the regulation of ENaC by uPA in primary mouse tracheal epithelial cells (MTE). The central hypothesis is that urokinase-like plasminogen activator (uPA) regulates ENaC function in airway epithelial cells. We found that both basal and cAMP-activated Na^+ flows through ENaC were significantly reduced in *uPA*-deficient cells. The reduction in ENaC activity was further confirmed in basolateral membrane permeabilized cells. A decrease in the Na^+/K^+-ATPase activity could contribute to the attenuation of ENaC function in intact monolayer cells. Dysfunctional fluid resolution was seen in *uPA*-disrupted cells. Administration of uPA and plasmin partially restores ENaC activity and fluid re-absorption by MTE cells. ERK1/2, but not Akt phosphorylation was observed in the cells and lungs of *uPA*-deficient mice. On the other hand, cleavage of γ ENaC is significantly depressed in the lungs of *uPA* knockout mice. Expression of caspase 8, an apoptosis molecule, however,

did not differ between wild type and *uPA*$^{-/-}$ mice. In addition, uPA deficiency did not alter transepithelial resistance. This is the first report demonstrating that urokinase up-regulates ENaC activity *in vivo* and *in vitro* (Chen *et al.*, 2014). These experiments were completed by collaborating with Drs. Chen, Zhao, Bhattarai, Dhiman, Shetty, and Idell.

The third set of experiments was to explore the underlying pharmacological mechanisms for uPA to up regulate ENaC. The hypothesis is that uPA may activate ENaC through proteolysis. My results show that two-chain urokinase (tcuPA) strongly stimulates heterologous human $\alpha\beta\gamma$ ENaC activity in a dose- and time-dependent manner. This activity of tcuPA was completely ablated by PAI-1. Furthermore, a mutation (S195A) of the active site of the enzyme also prevented ENaC activation. By comparison, three truncation mutants of the amino terminal fragment of tcuPA still activated ENaC. uPA enzymatic activity was positively correlated with ENaC current amplitude prior to reaching the maximal level. In sharp contrast to uPA, neither single-chain tPA nor derivatives, including tctPA and tenecteplase, affected ENaC activity. Furthermore, γ but not α ENaC subunit was proteolytically cleaved (^{177}GR↓KR^{180}) by tcuPA. In summary, the underlying mechanisms of urokinase-mediated activation of ENaC include release of self-inhibition, proteolysis of γ ENaC, incremental increase in opening rate, and activation of closed (electrically “silent”) channels. In addition, plasmin activated ENaC in a similar way. These studies for the first time demonstrate multifaceted mechanisms for fibrinolysin-mediated up-regulation of ENaC (Ji *et al.*, 2015), which form the cellular and molecular rationale for the beneficial effects of urokinase and plasmin in mitigating pulmonary oedema and pleural effusions. These

experiments were completed by collaborating with Drs. Zhao, Komissarov, Chang, Liu, and Matthay.

Finally, I characterized the potential mechanisms for the interactions between proteolysis and other external ligands, including inhibitory peptides, CPT-cGMP and cpt-cAMP (Nie *et al.*, 2010; Han *et al.*, 2011; Molina *et al.*, 2011). I hypothesized that serine proteases fully open the gate of ENaC channels, while other ENaC activators or external ligands partially stimulate channel activity. Our results show that CPT-cGMP and cpt-cAMP activate ENaC function through release of external sodium self-inhibition. In contrast, serine proteases cleave the extracellular loop of ENaC proteins and remove "inhibitory peptides", which is located closely to the first transmembrane domain. ENaC channels treated with serine proteins were on longer activated by these external ligands. In strict contrast, in the presence of CPT-cGMP or cpt-cAMP, serine proteases were able to activate ENaC activity to a maximal extent. Clearly, our studies demonstrate that proteases are the most potent ENaC activators. These experiments were completed by collaborating with Drs. Zhao, Komissarov, Chang, Liu, and Matthay.

Contributions to 4 of 105 publications

1. **Ji HL**, Zhao R, Komissarov AA, Chang Y, Liu Y, Matthay MA. Proteolytic regulation of epithelial sodium channels by urokinase plasminogen activator: cutting edge and cleavage sites. *Journal of Biological Chemistry*. 2015 Feb 27; 290(9): 5241-55. PMID: 25555911.

   Word count: 11,526.

   My contribution: 80%.

   The nature (role) of contributions: I initiated the concept, organized and coordinated team work, designed each experiment. All of functional evaluations using the two-electrode voltage clamp techniques and in silico analysis (Figures 1-4, 8A & B) were performed by myself. Immunoblotting assays and fibrinolysin activity were completed by the collaborators under my supervision (Figures 5-7, 8C & D). I also analysed each experiment, plotted all figures (Figures 1-9), drafted each version of the manuscript, submitted the paper and prepared responses to the reviewers' critiques. All of experiments were done within my laboratory.

2. Chen Z, Zhao R, Zhao M, Liang X, Bhattarai D, Dhiman R, Shetty S, Idell S, **Ji HL**. Regulation of epithelial sodium channels in urokinase plasminogen activator deficiency. *American Journal of Physiology Lung Cellular and Molecular Physiology*. 2014, Oct 15; 307(8): L609-17. PMID: 25172911.

Word count: 7,569.

My contribution: 60%.

The nature (role) of contributions: I initiated the concept, organized and coordinated team work, and designed each experiment. Ussing chamber experiments (Figures 1-3), and fluid height imaging (Figure 8), and Western blots (Figures 4-7) were performed by the collaborators under my supervision. All of the experiments were done in my laboratory. I analyzed all experiments, plotted figures, drafted each version of the manuscript, submitted the paper and prepared responses to the reviewers' critiques.

3. **Ji HL**, Zhao RZ, Shetty S, Idell S, Matalon S. Delta ENaC, a novel amiloride-inhibitible sodium channel. *American Journal of Physiology- Lung Cellular and Molecular Physiology*. 2012 Dec 15; 303(12): L1013-26. PMID: 22983350.

   Word count: 13,045.

   My contribution: 80%.

   The nature (role) of contributions: I initiated the concept, organized and coordinated team work, designed each section, searched and reviewed literature, plotted Figures 1-3, made Tables 1 and 2, drafted each version of the manuscript, submitted the paper and prepared responses to the reviewers' critiques. The collaborators revised the manuscript and discussed the structure of the paper.

4. Zhao RZ, Nie HG, Su XF, Han DY, Lee A, Huang Y, Chang Y, Matalon S, **Ji HL**. Characterization of a novel splice variant of δ ENaC subunit in human lungs. *American Journal of Physiology- Lung Cellular and Molecular Physiology*. 2012 Jun 15; 302(12): L1262-72. PMID: 22505667.

   Word count: 9,147.

   My contribution: 50%.

   The nature (role) of contributions: I initiated the project, organized and coordinated team work, and designed each experiment. I carried out functional studies in *Xenopus* oocytes (Figures 2-6). *In situ* hybridization, cloning, *in vitro* transcription, and blasting were done by the collaborators under my supervision (Figure 1). I also analysed each experiment, plotted all figures, drafted each version of the manuscript, submitted the paper and prepared responses to the reviewers' critiques with help of the collaborators.

Bibliography

Aleman C, Porcel JM, Alegre J, Ruiz E, Bielsa S, Andreu J, Deu M, Sune P, Martinez-Sogues M, Lopez I, Pallisa E, Schoenenberger JA, Bruno Montoro J & de Sevilla TF. (2015). Intrapleural fibrinolysis with urokinase versus alteplase in complicated parapneumonic pleural effusions and empyemas: A prospective randomized study. *Lung* **193,** 993-1000.

Andreasen D, Vuagniaux G, Fowler-Jaeger N, Hummler E & Rossier BC. (2006). Activation of epithelial sodium channels by mouse channel activating proteases (mCAP) expressed in *Xenopus* oocytes requires catalytic activity of mCAP3 and mCAP2 but not mCAP1. *J Am Soc Nephrol* **17,** 968-976.

Arias-Diaz J, Vara E, Torres-Melero J, Garcia C, Baki W, Ramirez-Armengol JA & Balibrea JL. (1994). Nitrite/nitrate and cytokine levels in bronchoalveolar lavage fluid of lung cancer patients. *Cancer* **74,** 1546.

Arteaga MF & Canessa CM. (2005). Functional specificity of Sgk1 and Akt1 on ENaC activity. *Am J Physiol Renal Physiol* **289,** F90-96.

Barazzone C, Belin D, Piguet PF, Vassalli JD & Sappino AP. (1996). Plasminogen activator inhibitor-1 in acute hyperoxic mouse lung injury. *J Clin Invest* **98,** 2666-2673.

Berthiaume Y & Matthay MA. (2007). Alveolar edema fluid clearance and acute lung injury. *Respir Physiol Neurobiol* **159,** 350-359.

Bertozzi P, Astedt B, Zenzius L, Lynch K, LeMaire F, Zapol W & Chapman HA, Jr. (1990). Depressed bronchoalveolar urokinase activity in patients with adult respiratory distress syndrome. *N Engl J Med* **322,** 890-897.

Bonny O, Chraibi A, Loffing J, Jaeger NF, Grunder S, Horisberger JD & Rossier BC. (1999). Functional expression of a pseudohypoaldosteronism type I mutated epithelial Na+ channel lacking the pore-forming region of its alpha subunit. *J Clin Invest* **104,** 967-974.

Boucher RC. (2007). Airway surface dehydration in cystic fibrosis: pathogenesis and therapy. *Annu Rev Med* **58,** 157-170.

Bubien JK, Cornwell T, Bradford AL, Fuller CM, DuVall MD & Benos DJ. (1998). Alpha-adrenergic receptors regulate human lymphocyte amiloride-sensitive sodium channels. *Am J Physiol* **275,** C702-710.

Bubien JK, Ismailov, II, Berdiev BK, Cornwell T, Lifton RP, Fuller CM, Achard JM, Benos DJ & Warnock DG. (1996). Liddle's disease: abnormal regulation of

amiloride-sensitive Na^+ channels by beta-subunit mutation. *Am J Physiol* **270,** C208-213.

Bubien JK, Watson B, Khan MA, Langloh AL, Fuller CM, Berdiev B, Tousson A & Benos DJ. (2001). Expression and regulation of normal and polymorphic epithelial sodium channel by human lymphocytes. *J Biol Chem* **276,** 8557-8566.

Caldwell RA, Boucher RC & Stutts MJ. (2004). Serine protease activation of near-silent epithelial Na^+ channels. *Am J Physiol Cell Physiol* **286,** C190-194.

Caldwell RA, Boucher RC & Stutts MJ. (2005). Neutrophil elastase activates near-silent epithelial Na^+ channels and increases airway epithelial Na^+ transport. *Am J Physiol Lung Cell Mol Physiol* **288,** L813-819.

Canessa CM, Horisberger JD & Rossier BC. (1993). Epithelial sodium channel related to proteins involved in neurodegeneration [see comments]. *Nature* **361,** 467-470.

Canessa CM, Schild L, Buell G, Thorens B, Gautschi I, Horisberger JD & Rossier BC. (1994). Amiloride-sensitive epithelial Na^+ channel is made of three homologous subunits. *Nature* **367,** 463-467.

Cao GQ, Li L, Wang YB, Shi ZZ, Fan DY & Chen HY. (2015). Treatment of free-flowing tuberculous pleurisy with intrapleural urokinase. *Int J Tuberc Lung Dis* **19,** 1395-1400.

Cases Viedma E, Lorenzo Dus MJ, Gonzalez-Molina A & Sanchis Aldas JL. (2006). A study of loculated tuberculous pleural effusions treated with intrapleural urokinase. *Respir Med* **100,** 2037-2042.

Chapman HA, Allen CL & Stone OL. (1986). Abnormalities in pathways of alveolar fibrin turnover among patients with interstitial lung disease. *Am Rev Respir Dis* **133,** 437-443.

Chen J, Kleyman TR & Sheng S. (2013). Gain-of-function variant of the human epithelial sodium channel. *Am J Physiol Renal Physiol* **304,** F207-213.

Chen L, Bosworth CA, Pico T, Collawn JF, Varga K, Gao Z, Clancy JP, Fortenberry JA, Lancaster JR, Jr. & Matalon S. (2008). DETANO and nitrated lipids increase chloride secretion across lung airway cells. *Am J Respir Cell Mol Biol* **39,** 150-162.

Chen L, Song W, Davis IC, Shrestha K, Schwiebert E, Sullender WM & Matalon S. (2009). Inhibition of Na^+ transport in lung epithelial cells by respiratory syncytial virus infection. *Am J Respir Cell Mol Biol* **40,** 588-600.

Chen Z, Zhao R, Zhao M, Liang X, Bhattarai D, Dhiman R, Shetty S, Idell S & Ji HL. (2014). Regulation of epithelial sodium channels in urokinase plasminogen activator deficiency. *Am J Physiol Lung Cell Mol Physiol* **307,** L609-617.

Chraibi A & Horisberger JD. (2002). Na self inhibition of human epithelial Na channel: temperature dependence and effect of extracellular proteases. *J Gen Physiol* **120,** 133-145.

Chraibi A, Schnizler M, Clauss W & Horisberger JD. (2001). Effects of 8-cpt-cAMP on the epithelial sodium channel expressed in *Xenopus* oocytes. *J Membr Biol* **183,** 15-23.

Czikora I, Alli A, Bao HF, Kaftan D, Sridhar S, Apell HJ, Gorshkov B, White R, Zimmermann A, Wendel A, Pauly-Evers M, Hamacher J, Garcia-Gabay I, Fischer B, Verin A, Bagi Z, Pittet JF, Shabbir W, Lemmens-Gruber R, Chakraborty T, Lazrak A, Matthay MA, Eaton DC & Lucas R. (2014). A novel tumor necrosis factor-mediated mechanism of direct epithelial sodium channel activation. *American Journal Of Respiratory And Critical Care Medicine* **190,** 522-532.

Davis IC & Matalon S. (2007). Epithelial sodium channels in the adult lung--important modulators of pulmonary health and disease. *Adv Exp Med Biol* **618,** 127-140.

Diacon AH, Theron J, Schuurmans MM, Van de Wal BW & Bolliger CT. (2004). Intrapleural streptokinase for empyema and complicated parapneumonic effusions. *Am J Respir Crit Care Med* **170,** 49-53.

Diakov A, Bera K, Mokrushina M, Krueger B & Korbmacher C. (2008). Cleavage in the gamma-subunit of the epithelial sodium channel (ENaC) plays an important role in the proteolytic activation of near-silent channels. *J Physiol* **586,** 4587-4608.

Du A, Zhao B, Yin D, Zhang S & Miao J. (2006). Safrole oxide induces apoptosis by activating caspase-3, -8, and -9 in A549 human lung cancer cells. *Bioorg Med Chem Lett* **16,** 81-83.

Eaton DC, Helms MN, Koval M, Bao HF & Jain L. (2009). The contribution of epithelial sodium channels to alveolar function in health and disease. *Annu Rev Physiol* **71,** 403-423.

Edelheit O, Ben-Shahar R, Dascal N, Hanukoglu A & Hanukoglu I. (2014). Conserved charged residues at the surface and interface of epithelial sodium channel subunits--roles in cell surface expression and the sodium self-inhibition response. *Febs J* **281,** 2097-2111.

Froudarakis ME, Kouliatsis G, Steiropoulos P, Anevlavis S, Pataka A, Popidou M, Mikroulis D, Pneumatikos I & Bouros D. (2008). Recombinant tissue plasminogen

activator in the treatment of pleural infections in adults. *Respir Med* **102,** 1694-1700.

Fuller CM, Ismailov, II, Berdiev BK, Shlyonsky VG & Benos DJ. (1996). Kinetic interconversion of rat and bovine homologs of the alpha subunit of an amiloride-sensitive Na^+ channel by C-terminal truncation of the bovine subunit. *J Biol Chem* **271,** 26602-26608.

Garty H & Benos DJ. (1988). Characteristics and regulatory mechanisms of the amiloride- blockable Na^+ channel. *PhysiolRev* **68,** 309.

Garty H & Palmer LG. (1997). Epithelial sodium channels: function, structure, and regulation. *Physiol Rev* **77,** 359-396.

Giraldez T, Dominguez J & Alvarez de la Rosa D. (2013). ENaC in the brain--future perspectives and pharmacological implications. *Curr Mol Pharmacol* **6,** 44-49.

Giraldez T, Rojas P, Jou J, Flores C & Alvarez de la Rosa D. (2012). The epithelial sodium channel delta-subunit: new notes for an old song. *Am J Physiol Renal Physiol* **303,** 9.

Glas GJ, Van Der Sluijs KF, Schultz MJ, Hofstra JJ, Van Der Poll T & Levi M. (2013). Bronchoalveolar hemostasis in lung injury and acute respiratory distress syndrome. *J Thromb Haemost* **11,** 17-25.

Goldfarb SB, Kashlan OB, Watkins JN, Suaud L, Yan W, Kleyman TR & Rubenstein RC. (2006). Differential effects of Hsc70 and Hsp70 on the intracellular trafficking and functional expression of epithelial sodium channels. *Proc Natl Acad Sci U S A* **103,** 5817-5822.

Gross TJ, Simon RH & Sitrin RG. (1990). Expression of urokinase-type plasminogen activator by rat pulmonary alveolar epithelial cells. *Am J Respir Cell Mol Biol* **3,** 449-456.

Haerteis S, Krappitz M, Diakov A, Krappitz A, Rauh R & Korbmacher C. (2012). Plasmin and chymotrypsin have distinct preferences for channel activating cleavage sites in the gamma subunit of the human epithelial sodium channel. *J Gen Physiol* **140,** 375-389.

Haerteis S, Krueger B, Korbmacher C & Rauh R. (2009). The delta-subunit of the epithelial sodium channel (ENaC) enhances channel activity and alters proteolytic ENaC activation. *J Biol Chem* **284,** 29024-29040.

Han DY, Nie HG, Gu X, Nayak RC, Su XF, Fu J, Chang Y, Rao V & Ji HL. (2010). K+ channel openers restore verapamil-inhibited lung fluid resolution and transepithelial ion transport. *Respir Res* **11,** 65.

Han DY, Nie HG, Su XF, Shi XM, Bhattarai D, Zhao M, Zhao RZ, Landers K, Tang H, Zhang L & Ji HL. (2011). 8-(4-chlorophenylthio)-guanosine-3',5'-cyclic monophosphate-Na stimulates human alveolar fluid clearance by releasing external Na^+ self-inhibition of epithelial Na^+ channels. *Am J Respir Cell Mol Biol* **45,** 1007-1014.

Hanukoglu I & Hanukoglu A. (2016). Epithelial sodium channel (ENaC) family: Phylogeny, structure-function, tissue distribution, and associated inherited diseases. *Gene* **579,** 95-132.

Hardiman KM, Nicholas-Bevensee CM, Fortenberry J, Myles CT, Malik B, Eaton DC & Matalon S. (2004). Regulation of amiloride-sensitive Na^+ transport by basal nitric oxide. *AmJRespirCell MolBiol* **30,** 720.

Hildenbrand R, Gandhari M, Stroebel P, Marx A, Allgayer H & Arens N. (2008). The urokinase-system--role of cell proliferation and apoptosis. *Histol Histopathol* **23,** 227-236.

Hobbs CA, Da Tan C & Tarran R. (2013). Does epithelial sodium channel hyperactivity contribute to cystic fibrosis lung disease? *J Physiol* **591,** 4377-4387.

Huang LT, Chou HC, Wang LF & Chen CM. (2012). Tissue plasminogen activator attenuates ventilator-induced lung injury in rats. *Acta Pharmacol Sin* **33,** 991-997.

Hummler E, Barker P, Gatzy J, Beermann F, Verdumo C, Schmidt A, Boucher R & Rossier BC. (1996). Early death due to defective neonatal lung liquid clearance in alpha ENaC -deficient mice. *Nat Genet* **12,** 325-328.

Hummler E & Planes C. (2010). Importance of ENaC-mediated sodium transport in alveolar fluid clearance using genetically-engineered mice. *Cell Physiol Biochem* **25,** 63-70.

Hummler E & Vallon V. (2005). Lessons from mouse mutants of epithelial sodium channel and its regulatory proteins. *J Am Soc Nephrol* **16,** 3160-3166.

Idell S. (2003). Coagulation, fibrinolysis, and fibrin deposition in acute lung injury. *Crit Care Med* **31,** S213-220.

Idell S. (2008). The pathogenesis of pleural space loculation and fibrosis. *Curr Opin Pulm Med* **14,** 310-315.

Idell S, James KK & Coalson JJ. (1992a). Fibrinolytic activity in bronchoalveolar lavage of baboons with diffuse alveolar damage: trends in two forms of lung injury. *Crit Care Med* **20,** 1431-1440.

Idell S, Koenig KB, Fair DS, Martin TR, McLarty J & Maunder RJ. (1991). Serial abnormalities of fibrin turnover in evolving adult respiratory distress syndrome. *Am J Physiol* **261,** L240-248.

Idell S, Zwieb C, Kumar A, Koenig KB & Johnson AR. (1992b). Pathways of fibrin turnover of human pleural mesothelial cells in vitro. *Am J Respir Cell Mol Biol* **7,** 414-426.

Itani OA, Auerbach SD, Husted RF, Volk KA, Ageloff S, Knepper MA, Stokes JB & Thomas CP. (2002). Glucocorticoid-stimulated lung epithelial Na^+ transport is associated with regulated ENaC and sgk1 expression. *Am J Physiol Lung Cell Mol Physiol* **282,** L631-641.

Jain L, Chen XJ, Brown LA & Eaton DC. (1998). Nitric oxide inhibits lung sodium transport through a cGMP-mediated inhibition of epithelial cation channels. *Am J Physiol* **274,** L475-484.

Jasti J, Furukawa H, Gonzales EB & Gouaux E. (2007). Structure of acid-sensing ion channel 1 at 1.9 A resolution and low pH. *Nature* **449,** 316-323.

Ji HL & Benos DJ. (2004). Degenerin sites mediate proton activation of deltabetagamma-epithelial sodium channel. *J Biol Chem* **279,** 26939-26947.

Ji HL, Bishop LR, Anderson SJ, Fuller CM & Benos DJ. (2004). The role of pre-H2 domains of alpha- and delta-epithelial Na^+ channels in ion permeation, conductance, and amiloride sensitivity. *J Biol Chem* **279,** 8428-8440.

Ji HL, Chalfant ML, Jovov B, Lockhart JP, Parker SB, Fuller CM, Stanton BA & Benos DJ. (2000). The cytosolic termini of the beta- and gamma-ENaC subunits are involved in the functional interactions between cystic fibrosis transmembrane conductance regulator and epithelial sodium channel. *J Biol Chem* **275,** 27947-27956.

Ji HL, DuVall MD, Patton HK, Satterfield CL, Fuller CM & Benos DJ. (1998a). Functional expression of a truncated Ca^{2+}-activated Cl^- channel and activation by phorbol ester. *Am J Physiol* **274,** C455-464.

Ji HL, Fuller CM & Benos DJ. (1998b). Osmotic pressure regulates alpha beta gamma-rENaC expressed in *Xenopus* oocytes. *Am J Physiol* **275,** C1182-1190.

Ji HL, Fuller CM & Benos DJ. (1999). Peptide inhibition of constitutively activated epithelial Na^+ channels expressed in *Xenopus* oocytes. *J Biol Chem* **274,** 37693-37704.

Ji HL, Fuller CM & Benos DJ. (2002a). Intrinsic gating mechanisms of epithelial sodium channels. *Am J Physiol Cell Physiol* **283,** C646-650.

Ji HL, Jovov B, Fu J, Bishop LR, Mebane HC, Fuller CM, Stanton BA & Benos DJ. (2002b). Up-regulation of acid-gated Na^+ channels (ASICs) by cystic fibrosis transmembrane conductance regulator co-expression in *Xenopus* oocytes. *J Biol Chem* **277,** 8395-8405.

Ji HL, Parker S, Langloh AL, Fuller CM & Benos DJ. (2001). Point mutations in the post-M2 region of human alpha-ENaC regulate cation selectivity. *Am J Physiol Cell Physiol* **281,** C64-74.

Ji HL, Su XF, Kedar S, Li J, Barbry P, Smith PR, Matalon S & Benos DJ. (2006). Delta-subunit confers novel biophysical features to alpha beta gamma-human epithelial sodium channel (ENaC) via a physical interaction. *J Biol Chem* **281,** 8233-8241.

Ji HL, Zhao R, Komissarov AA, Chang Y, Liu Y & Matthay MA. (2015). Proteolytic regulation of epithelial sodium channels by urokinase plasminogen activator: cutting edge and cleavage sites. *J Biol Chem* **290,** 5241-5255.

Ji HL, Zhao RZ, Chen ZX, Shetty S, Idell S & Matalon S. (2012). delta ENaC: a novel divergent amiloride-inhibitable sodium channel. *Am J Physiol Lung Cell Mol Physiol* **303,** L1013-1026.

Jovov B, Berdiev BK, Fuller CM, Ji HL & Benos DJ. (2002). The serine protease trypsin cleaves C termini of beta- and gamma-subunits of epithelial Na^+ channels. *J Biol Chem* **277,** 4134-4140.

Ke SH, Coombs GS, Tachias K, Corey DR & Madison EL. (1997a). Optimal subsite occupancy and design of a selective inhibitor of urokinase. *J Biol Chem* **272,** 20456-20462.

Ke SH, Coombs GS, Tachias K, Navre M, Corey DR & Madison EL. (1997b). Distinguishing the specificities of closely related proteases. Role of P3 in substrate and inhibitor discrimination between tissue-type plasminogen activator and urokinase. *J Biol Chem* **272,** 16603-16609.

Kellenberger S & Schild L. (2002). Epithelial sodium channel/degenerin family of ion channels: a variety of functions for a shared structure. *Physiol Rev* **82,** 735-767.

Kemp PJ, Kim KJ, Borok Z & Crandall ED. (2001). Re-evaluating the Na^+ conductance of adult rat alveolar type II pneumocytes: evidence for the involvement of cGMP-activated cation channels. *J Physiol* **536,** 693-701.

Kleyman TR, Carattino MD & Hughey RP. (2009). ENaC at the cutting edge: regulation of epithelial sodium channels by proteases. *J Biol Chem* **284,** 20447-20451.

Kleyman TR & Cragoe EJ, Jr. (1988). The mechanism of action of amiloride. *Semin Nephrol* **8,** 242-248.

Kleyman TR, Sheng S, Kosari F & Kieber-Emmons T. (1999). Mechanism of action of amiloride: a molecular prospective. *Semin Nephrol* **19,** 524-532.

Komissarov AA, Florova G, Azghani A, Karandashova S, Kurdowska AK & Idell S. (2013). Active alpha-macroglobulin is a reservoir for urokinase after fibrinolytic therapy in rabbits with tetracycline-induced pleural injury and in human pleural fluids. *Am J Physiol Lung Cell Mol Physiol* **305,** L682-692.

Kotani I, Sato A, Hayakawa H, Urano T, Takada Y & Takada A. (1995). Increased procoagulant and antifibrinolytic activities in the lungs with idiopathic pulmonary fibrosis. *Thromb Res* **77,** 493-504.

Kulaksiz H, Schmid A, Honscheid M, Ramaswamy A & Cetin Y. (2002). Clara cell impact in air-side activation of CFTR in small pulmonary airways. *ProcNatlAcadSciUSA* **99,** 6796.

Lazrak A, Chen L, Jurkuvenaite A, Doran SF, Liu G, Li Q, Lancaster JR, Jr. & Matalon S. (2012). Regulation of alveolar epithelial Na^+ channels by ERK1/2 in chlorine-breathing mice. *Am J Respir Cell Mol Biol* **46,** 342-354.

Lazrak A, Jurkuvenaite A, Chen L, Keeling KM, Collawn JF, Bedwell DM & Matalon S. (2011). Enhancement of alveolar epithelial sodium channel activity with decreased cystic fibrosis transmembrane conductance regulator expression in mouse lung. *Am J Physiol Lung Cell Mol Physiol* **301,** L557-567.

Lazrak A & Matalon S. (2003). cAMP-induced changes of apical membrane potentials of confluent H441 monolayers. *Am J Physiol Lung Cell Mol Physiol* **285,** L443-450.

Lazrak A, Nita I, Subramaniyam D, Wei S, Song W, Ji HL, Janciauskiene S & Matalon S. (2009). Alpha(1)-antitrypsin inhibits epithelial Na^+ transport in vitro and in vivo. *Am J Respir Cell Mol Biol* **41,** 261-270.

Lee IH, Dinudom A, Sanchez-Perez A, Kumar S & Cook DI. (2007). Akt mediates the effect of insulin on epithelial sodium channels by inhibiting Nedd4-2. *J Biol Chem* **282,** 29866-29873.

Maarouf AB, Sheng N, Chen J, Winarski KL, Okumura S, Carattino MD, Boyd CR, Kleyman TR & Sheng S. (2009). Novel determinants of epithelial sodium channel gating within extracellular thumb domains. *J Biol Chem* **284,** 7756-7765.

Mall M, Grubb BR, Harkema JR, O'Neal WK & Boucher RC. (2004). Increased airway epithelial Na+ absorption produces cystic fibrosis-like lung disease in mice. *Nat Med* **10,** 487-493.

Mall MA. (2016). Unplugging mucus in cystic fibrosis and chronic obstructive pulmonary disease. *Ann Am Thorac Soc* **13 Suppl 2,** S177-185.

Mall MA, Button B, Johannesson B, Zhou Z, Livraghi A, Caldwell RA, Schubert SC, Schultz C, O'Neal WK, Pradervand S, Hummler E, Rossier BC, Grubb BR & Boucher RC. (2010). Airway surface liquid volume regulation determines different airway phenotypes in liddle compared with betaENaC-overexpressing mice. *J Biol Chem* **285,** 26945-26955.

Mall MA, Harkema JR, Trojanek JB, Treis D, Livraghi A, Schubert S, Zhou Z, Kreda SM, Tilley SL, Hudson EJ, O'Neal WK & Boucher RC. (2008). Development of chronic bronchitis and emphysema in beta-epithelial Na^+ channel-overexpressing mice. *Am J Respir Crit Care Med* **177,** 730-742.

Marhuenda C, Barcelo C, Fuentes I, Guillen G, Cano I, Lopez M, Hernandez F, Perez-Yarza EG, Matute JA, Garcia-Casillas MA, Alvarez V & Moreno-Galdo A. (2014). Urokinase versus VATS for treatment of empyema: a randomized multicenter clinical trial. *Pediatrics* **134,** e1301-1307.

Marshall BC, Sageser DS, Rao NV, Emi M & Hoidal JR. (1990). Alveolar epithelial cell plasminogen activator. Characterization and regulation. *J Biol Chem* **265,** 8198-8204.

Matalon S, Bartoszewski R & Collawn JF. (2015). Role of epithelial sodium channels (ENaC) in the regulation of lung fluid homeostasis. *Am J Physiol Lung Cell Mol Physiol* **309,** L1229-L1238.

Matalon S, Lazrak A, Jain L & Eaton DC. (2002). Invited review: biophysical properties of sodium channels in lung alveolar epithelial cells. *J Appl Physiol (1985)* **93,** 1852-1859.

Matalon S & O'Brodovich H. (1999). Sodium channels in alveolar epithelial cells: molecular characterization, biophysical properties, and physiological significance. *Annu Rev Physiol* **61,** 627-661.

Matthay MA. (2014). Resolution of pulmonary edema. Thirty years of progress. *Am J Respir Crit Care Med* **189,** 1301-1308.

Matthay MA, Folkesson HG & Clerici C. (2002). Lung epithelial fluid transport and the resolution of pulmonary edema. *Physiol Rev* **82,** 569-600.

Matthay MA, Robriquet L & Fang X. (2005). Alveolar epithelium: role in lung fluid balance and acute lung injury. *Proc Am Thorac Soc* **2,** 206-213.

McMahon B & Kwaan HC. (2008). The plasminogen activator system and cancer. *Pathophysiol Haemost Thromb* **36,** 184-194.

Meyer G, Vicaut E, Danays T, Agnelli G, Becattini C, Beyer-Westendorf J, Bluhmki E, Bouvaist H, Brenner B, Couturaud F, Dellas C, Empen K, Franca A, Galie N, Geibel A, Goldhaber SZ, Jimenez D, Kozak M, Kupatt C, Kucher N, Lang IM, Lankeit M, Meneveau N, Pacouret G, Palazzini M, Petris A, Pruszczyk P, Rugolotto M, Salvi A, Schellong S, Sebbane M, Sobkowicz B, Stefanovic BS, Thiele H, Torbicki A, Verschuren F & Konstantinides SV. (2014). Fibrinolysis for patients with intermediate-risk pulmonary embolism. *N Engl J Med* **370,** 1402-1411.

Molina R, Han DY, Su XF, Zhao RZ, Zhao M, Sharp GM, Chang Y & Ji HL. (2011). Cpt-cAMP activates human epithelial sodium channels via relieving self-inhibition. *Biochim Biophys Acta* **1808,** 1818-1826.

Mukherjee A, Mueller GM, Kinlough CL, Sheng N, Wang Z, Mustafa SA, Kashlan OB, Kleyman TR & Hughey RP. (2014). Cysteine palmitoylation of the gamma subunit has a dominant role in modulating activity of the epithelial sodium channel. *J Biol Chem* **289,** 14351-14359.

Munster AM, Bendstrup E, Jensen JI & Gram J. (2000). Jet and ultrasonic nebulization of single chain urokinase plasminogen activator (scu-PA). *J Aerosol Med* **13,** 325-333.

Neitzel JJ. (2010). Enzyme catalysis: the serine proteases. *Nat Educ* **3,** 21.

Nie HG, Chen L, Han DY, Li J, Song WF, Wei SP, Fang XH, Gu X, Matalon S & Ji HL. (2009a). Regulation of epithelial sodium channels by cGMP/PKGII. *J Physiol* **587,** 2663-2676.

Nie HG, Tucker T, Su XF, Na T, Peng JB, Smith PR, Idell S & Ji HL. (2009b). Expression and regulation of epithelial Na^+ channels by nucleotides in pleural mesothelial cells. *Am J Respir Cell Mol Biol* **40,** 543-554.

Nie HG, Zhang W, Han DY, Li QN, Li J, Zhao RZ, Su XF, Peng JB & Ji HL. (2010). 8-pCPT-cGMP stimulates alphabetagamma-ENaC activity in oocytes as an external ligand requiring specific nucleotide moieties. *Am J Physiol Renal Physiol* **298,** F323-334.

Nishiuma T, Sisson TH, Subbotina N & Simon RH. (2004). Localization of plasminogen activator activity within normal and injured lungs by *in situ* zymography. *Am J Respir Cell Mol Biol* **31,** 552-558.

Passero CJ, Mueller GM, Rondon-Berrios H, Tofovic SP, Hughey RP & Kleyman TR. (2008). Plasmin activates epithelial Na^+ channels by cleaving the gamma subunit. *J Biol Chem* **283,** 36586-36591.

Piazza G, Hohlfelder B, Jaff MR, Ouriel K, Engelhardt TC, Sterling KM, Jones NJ, Gurley JC, Bhatheja R, Kennedy RJ, Goswami N, Natarajan K, Rundback J, Sadiq IR, Liu SK, Bhalla N, Raja ML, Weinstock BS, Cynamon J, Elmasri FF, Garcia MJ, Kumar M, Ayerdi J, Soukas P, Kuo W, Liu PY & Goldhaber SZ. (2015). A prospective, single-arm, multicenter trial of ultrasound-facilitated, catheter-directed, low-dose fibrinolysis for acute massive and submassive pulmonary embolism: The SEATTLE II study. *JACC Cardiovas Interventions* **8,** 1382-1392.

Planes C & Caughey GH. (2007). Regulation of the epithelial Na^+ channel by peptidases. *Curr Top Dev Biol* **78,** 23-46.

Prabhakaran P, Ware LB, White KE, Cross MT, Matthay MA & Olman MA. (2003). Elevated levels of plasminogen activator inhibitor-1 in pulmonary edema fluid are associated with mortality in acute lung injury. *Am J Physiol Lung Cell Mol Physiol* **285,** L20-28.

Prager GW, Mihaly J, Brunner PM, Koshelnick Y, Hoyer-Hansen G & Binder BR. (2009). Urokinase mediates endothelial cell survival via induction of the X-linked inhibitor of apoptosis protein. *Blood* **113,** 1383-1390.

Rahman NM, Maskell NA, West A, Teoh R, Arnold A, Mackinlay C, Peckham D, Davies CW, Ali N, Kinnear W, Bentley A, Kahan BC, Wrightson JM, Davies HE, Hooper CE, Lee YC, Hedley EL, Crosthwaite N, Choo L, Helm EJ, Gleeson FV, Nunn AJ & Davies RJ. (2011). Intrapleural use of tissue plasminogen activator and DNase in pleural infection. *N Engl J Med* **365,** 518-526.

Renauld S, Allache R & Chraibi C. (2008). Ile481 from the guinea pig alpha-subunit plays a major role in the activation of ENaC by cpt-cAMP. *Cell Physiol Biochem* **22,** 101-108.

Renckens R, Roelofs JJ, Stegenga ME, Florquin S, Levi M, Carmeliet P, Van't Veer C & van der Poll T. (2008). Transgenic tissue-type plasminogen activator expression improves host defense during Klebsiella pneumonia. *J Thromb Haemost* **6,** 660-668.

Rossier BC. (2004). The epithelial sodium channel: activation by membrane-bound serine proteases. *Proc Am Thorac Soc* **1,** 4-9.

Rossier BC & Stutts MJ. (2009). Activation of the epithelial sodium channel (ENaC) by serine proteases. *Annu Rev Physiol* **71,** 361-379.

Sakuma T, Zhao Y, Sugita M, Sagawa M, Toga H, Ishibashi T, Nishio M & Matthay MA. (2004). Malnutrition impairs alveolar fluid clearance in rat lungs. *A J Physiol Lung Cell Mol Physiol* **286,** L1268-1274.

Sandera P, Hillinger S, Stammberger U, Schoedon G, Zalunardo M, Weder W & Schmid RA. (2000). 8-Br-cyclic GMP given during reperfusion improves post-transplant lung edema and free radical injury. *Journal of Heart & Lung Transplantation* **19,** 173-178.

Sapru A, Curley MA, Brady S, Matthay MA & Flori H. (2010). Elevated PAI-1 is associated with poor clinical outcomes in pediatric patients with acute lung injury. *Intensive Care Med* **36,** 157-163.

Saydam O, Karapinar K, Gokce M, Kilic L, Metin M, Oz, II & Tanriverdi O. (2015). The palliative treatment with intrapleural streptokinase in patients with multiloculated malignant pleural effusion: a double-blind, placebo-controlled, randomized study. *Med Oncol* **32,** 612.

Sebag SC, Bastarache JA & Ware LB. (2011). Therapeutic modulation of coagulation and fibrinolysis in acute lung injury and the acute respiratory distress syndrome. *Curr Pharm Biotechnol* **12,** 1481-1496.

Sheng S, Maarouf AB, Bruns JB, Hughey RP & Kleyman TR. (2007). Functional role of extracellular loop cysteine residues of the epithelial Na^+ channel in Na^+ self-inhibition. *J Biol Chem* **282,** 20180-20190.

Sheng S, Perry CJ & Kleyman TR. (2002). External nickel inhibits epithelial sodium channel by binding to histidine residues within the extracellular domains of alpha and gamma subunits and reducing channel open probability. *J Biol Chem* **277,** 50098-50111.

Sheng S, Perry CJ & Kleyman TR. (2004). Extracellular Zn^{2+} activates epithelial Na^+ channels by eliminating Na^+ self-inhibition. *J Biol Chem* **279,** 31687-31696.

Shetty S, Padijnayayveetil J, Tucker T, Stankowska D & Idell S. (2008). The fibrinolytic system and the regulation of lung epithelial cell proteolysis, signaling, and cellular viability. *Am J Physiol Lung Cell Mol Physiol* **295,** L967-975.

Sisson TH, Hanson KE, Subbotina N, Patwardhan A, Hattori N & Simon RH. (2002). Inducible lung-specific urokinase expression reduces fibrosis and mortality after lung injury in mice. *Am J Physiol Lung Cell Mol Physiol* **283,** L1023-1032.

Sisson TH & Simon RH. (2007). The plasminogen activation system in lung disease. *Curr Drug Targets* **8,** 1016-1029.

Smith HW & Marshall CJ. (2010). Regulation of cell signalling by uPAR. *Nat Rev Mol Cell Biol* **11,** 23-36.

Stockand JD, Staruschenko A, Pochynyuk O, Booth RE & Silverthorn DU. (2008). Insight toward epithelial Na^+ channel mechanism revealed by the acid-sensing ion channel 1 structure. *IUBMB Life* **60,** 620-628.

Strange C, Baumann MH, Sahn SA & Idell S. (1995). Effects of intrapleural heparin or urokinase on the extent of tetracycline-induced pleural disease. *Am J Respir Crit Care Med* **151,** 508-515.

Stringer KA, Dunn JS & Gustafson DL. (2004). Administration of exogenous tissue plasminogen activator reduces oedema in mice lacking the tissue plasminogen activator gene. *Clin Exp Pharmacol Physiol* **31,** 327-330.

Stringer KA, Hybertson BM, Cho OJ, Cohen Z & Repine JE. (1998). Tissue plasminogen activator (tPA) inhibits interleukin-1 induced acute lung leak. *Free Radic Biol Med* **25,** 184-188.

Svenningsen P, Bistrup C, Friis UG, Bertog M, Haerteis S, Krueger B, Stubbe J, Jensen ON, Thiesson HC, Uhrenholt TR, Jespersen B, Jensen BL, Korbmacher C & Skott O. (2009a). Plasmin in nephrotic urine activates the epithelial sodium channel. *J Am Soc Nephrol* **20,** 299-310.

Svenningsen P, Uhrenholt TR, Palarasah Y, Skjodt K, Jensen BL & Skott O. (2009b). Prostasin-dependent activation of epithelial Na^+ channels by low plasmin concentrations. *Am J Physiol Regul Integr Comp Physiol* **297,** R1733-1741.

Takahashi K, Kiguchi T, Sawasaki Y, Karikusa F, Nemoto N, Matsuoka T & Yamamoto M. (1992). Lung capillary endothelial cells produce and secrete urokinase-type plasminogen activator. *Am J Respir Cell Mol Biol* **7,** 90-94.

Tarran R, Button B, Picher M, Paradiso AM, Ribeiro CM, Lazarowski ER, Zhang L, Collins PL, Pickles RJ, Fredberg JJ & Boucher RC. (2005). Normal and cystic fibrosis airway surface liquid homeostasis. The effects of phasic shear stress and viral infections. *J Biol Chem* **280,** 35751-35759.

Thome UH, Davis IC, Nguyen SV, Shelton BJ & Matalon S. (2003). Modulation of sodium transport in fetal alveolar epithelial cells by oxygen and corticosterone. *Am J Physiol Lung Cell Mol Physiol* **284,** L376-385.

Thommi G, Nair CK, Aronow WS, Shehan C, Meyers P & McLeay M. (2007). Efficacy and safety of intrapleural instillation of alteplase in the management of complicated pleural effusion or empyema. *Am J Ther* **14,** 341-345.

Thommi G, Shehan JC, Robison KL, Christensen M, Backemeyer LA & McLeay MT. (2012). A double blind randomized cross over trial comparing rate of decortication and efficacy of intrapleural instillation of alteplase *vs* placebo in patients with empyemas and complicated parapneumonic effusions. *Respir Med* **106,** 716-723.

Trautmann U & Pfeiffer RA. (1994). Interstitial deletion 12p13.1-13.3 in a mildly retarded infant with unilateral ectrodactyly. *Ann Genet* **37,** 147-149.

Tucker JK, Tamba K, Lee YJ, Shen LL, Warnock DG & Oh Y. (1998). Cloning and functional studies of splice variants of the alpha-subunit of the amiloride-sensitive Na^+ channel. *Am J Physiol* **274,** C1081-1089.

Tucker T & Idell S. (2013). Plasminogen-plasmin system in the pathogenesis and treatment of lung and pleural injury. *Semin Thromb Hemost* **39,** 373-381.

Unique. (2008). 1p36 deletion 2008. www.rarechromo.org/information/chromosome%20%201/1p36%20deletion%20ftnw.pdf.

Verspurten J, Gevaert K, Declercq W & Vandenabeele P. (2009). SitePredicting the cleavage of proteinase substrates. *Trends Biochem Sci* **34,** 319-323.

Viscardi RM, Broderick K, Sun CC, Yale-Loehr AJ, Hessamfar A, Taciak V, Burke KC, Koenig KB & Idell S. (1992). Disordered pathways of fibrin turnover in lung lavage of premature infants with respiratory distress syndrome. *Am Rev Respir Dis* **146,** 492-499.

Waldmann R, Champigny G, Bassilana F, Voilley N & Lazdunski M. (1995). Molecular cloning and functional expression of a novel amiloride-sensitive Na^+ channel. *J Biol Chem* **270,** 27411-27414.

Wang C, Zhai Z, Yang Y, Wu Q, Cheng Z, Liang L, Dai H, Huang K, Lu W, Zhang Z, Cheng X & Shen YH. (2010). Efficacy and safety of low dose recombinant tissue-type plasminogen activator for the treatment of acute pulmonary thromboembolism: a randomized, multicenter, controlled trial. *Chest* **137,** 254-262.

Wodopia R, Ko HS, Billian J, Wiesner R, Bartsch P & Mairbaurl H. (2000). Hypoxia decreases proteins involved in epithelial electrolyte transport in A549 cells and rat lung. *Am J Physiol Lung Cell Mol Physiol* **279,** L1110-1119.

Zhao R, Liang X, Zhao M, Liu SL, Huang Y, Idell S, Li X & Ji HL. (2014). Correlation of apical fluid-regulating channel proteins with lung function in human COPD lungs. *PLoS One* **9,** e109725.

Zhao RZ, Nie HG, Su XF, Han DY, Lee A, Huang Y, Chang Y, Matalon S & Ji HL. (2012). Characterization of a novel splice variant of delta ENaC subunit in human lungs. *Am J Physiol Lung Cell Mol Physiol* **302,** L1262-1272.

Zhou Z, Duerr J, Johannesson B, Schubert SC, Treis D, Harm M, Graeber SY, Dalpke A, Schultz C & Mall MA. (2011). The ENaC-overexpressing mouse as a model of cystic fibrosis lung disease. *J Cyst Fibros* **10 Suppl 2,** S172-182.

Zhou Z, Treis D, Schubert S, Harm M, Schatterny J, Hirtz S, Duerr J, Boucher RC & Mall MA. (2007). Preventive but not late ENaC blocker therapy reduces mortality and morbidity of cystic fibrosis-like lung disease in mice. *Pediatr Pulmonol* **30,** 294-294.

Zuckerman DA, Reed MF, Howington JA & Moulton JS. (2009). Efficacy of intrapleural tissue-type plasminogen activator in the treatment of loculated parapneumonic effusions. *J Vasc Interv Radiol* **20,** 1066-1069.